662160

DP-1690

PROCESS CONTROL FOR A CONTINUOUS URANYL NITRATE EVAPORATOR

S. F. PETERSON
L. P. MacINTYRE

SRL FILE
RECORD COPY

E. I. du Pont de Nemours & Co.
Savannah River Laboratory
Aiken, SC 29808

PREPARED FOR THE U. S. DEPARTMENT OF ENERGY UNDER CONTRACT DE-AC09-76SR00001

Printed in the United States of America

Available from

National Technical Information Service
U. S. Department of Commerce
5285 Port Royal Road
Springfield, Virginia 22161

Price: Printed Copy A05; Microfiche A01

662160

DP-1690

Distribution Category: UC-10

PROCESS CONTROL FOR A CONTINUOUS URANYL NITRATE EVAPORATOR

S. F. Peterson
L. P. MacIntyre

Approved by C. E. Coffey

Publication Date: July 1984

E. I. du Pont de Nemours & Co.
Savannah River Laboratory
Aiken, SC 29808

PREPARED FOR THE U. S. DEPARTMENT OF ENERGY UNDER CONTRACT DE AC09-76SR00001

ABSTRACT

A continuous uranyl nitrate evaporator at the Savannah River Plant (SRP) in Aiken, South Carolina was the subject of this work. A rigorous mathematical model of the evaporator was developed. A difference equation form of the model was then constructed and used for control studies.

Relative gain analysis was done on the system in order to identify any promising multivariable control schemes. Several alternate control schemes were modeled, tuned, and compared against the scheme presently in use at SRP.

As the pneumatic specific gravity instrumentation at SRP is very noisy, the noise was simulated and used in the second phase of the control study. In this phase, alternate tuning methods and filters were investigated and compared.

The control studies showed that the control algorithm now in use at SRP is the simplest and best available.

CONTENTS

CONTENTS, Contd

PROCESS CONTROL FOR A CONTINUOUS URANYL NITRATE EVAPORATOR

BACKGROUND

An evaporator used to concentrate aqueous uranyl nitrate solutions at the Savannah River Plant (SRP) in Aiken, SC was the subject of this investigation. The evaporator control study was chosen over several projects after taking into consideration the complexity and usefulness of the various projects to the company. This study is part of a large project to automate the Uranium-Plutonium Processing Facility at SRP. It was the aim of this project to choose the best control strategy for the evaporator. The primary control objective is to control the composition of the concentrate. It is necessary to ensure that no radioactivity escapes into the condenser. It is also desired to conserve energy where practical. Instrumentation is also a concern here, as the process solutions are highly radioactive, and the equipment must be operated remotely. From this, it follows that servicing faulty components is difficult. Therefore, instrumentation must be chosen that is particularly trouble-free.

A survey was made of related literature to find what direction past modelers had taken and what control methods had been tried and which methods worked best. A computer data base search for related literature was made using the Department of Energy (DOE) Energy Database, the Lockheed Engineering Database, and the DOE Central Inventory of Models. The Applied Science and Technology Index from 1965 to 1982, as well as the entire Computer and Control Abstracts were also searched for related articles.

Bacon and Howe

David Bacon of Queens University and Gerald Howe of Millhaven Fibres published a control study of a falling film evaporator at Chemcell Ltd.[1] In the original control scheme, as shown in Figure 1, the recycle was under flow control, the steam flow was under liquid temperature control, and the liquid flow rate was under liquid level control. All controllers were independent and all setpoints were constant. The Auto-Correlation factor and the Box-Pierce statistic (a white noise comparison) were used to evaluate control of the evaporator.

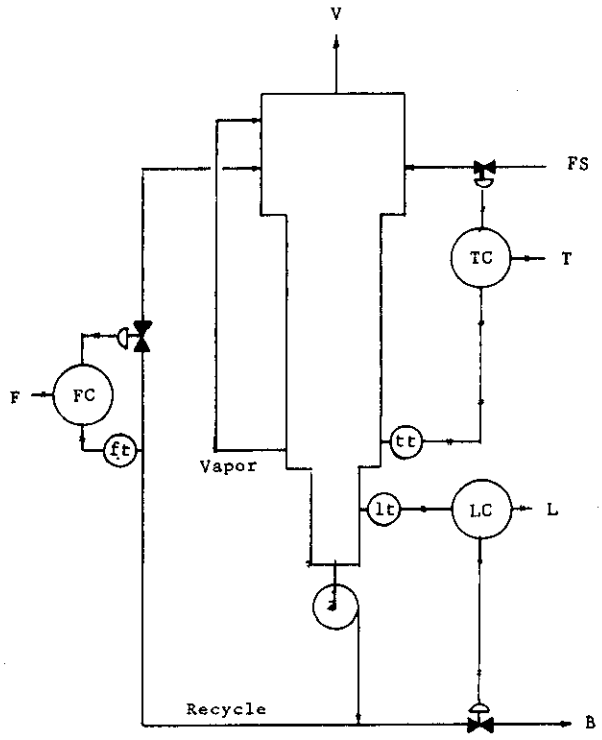

FIGURE 1. Falling Film Evaporator at Queens University

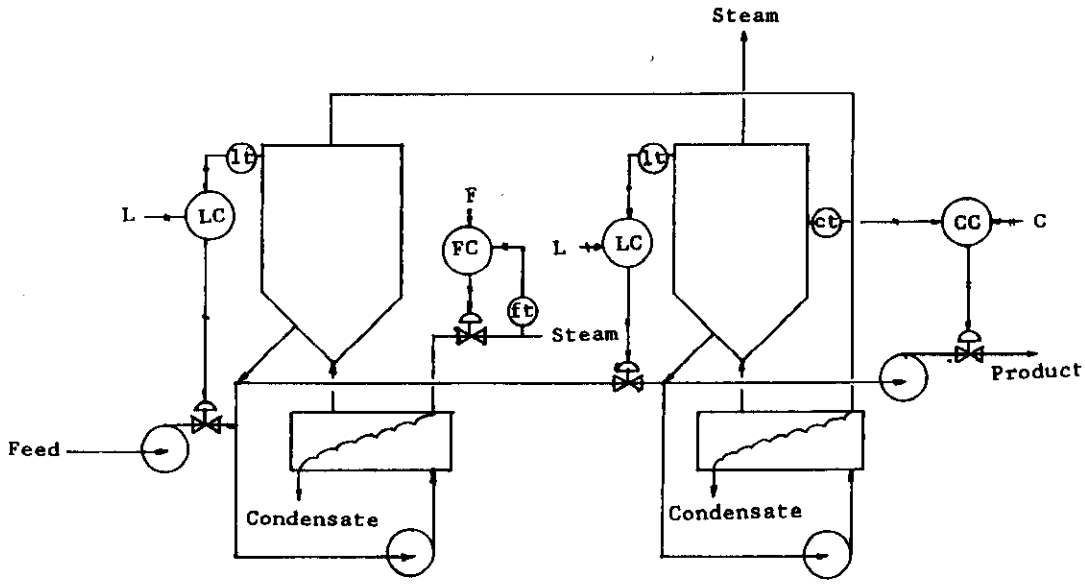

FIGURE 2. Quadruple-Effect Evaporator at Diamond Shamrock

A purely empirical model incorporating instrument noise was developed. The primary control variable was chosen as the liquid flow rate. It was determined that the liquid temperature and the liquid level were the only input variables that exhibited significant effects on the liquid flow rate. Under the present configuration, the liquid level could only be affected by using the liquid flow rate. This meant that the liquid temperature had to be used to control the liquid flow rate. This was possible, since the liquid temperature could be used to control the liquid composition, which could, in turn, control the liquid flow rate.

It was also determined that the recycle flow rate was the only monitored variable which could be used to control the temperature. Thus, the proposed control scheme was:

1. To leave the existing level control as it was.

2. To use the existing temperature control as a "slave" loop, with liquid flow rate as the "master" control.

3. To use the existing recycle flow control as a "slave" loop, with the deviation from the temperature setpoint used as the "master" loop.

The set point of the master loop was to be zero. A forty-fold improvement in variance was predicted from the stochastic model using the additional control, but no actual test data were reported.

Harvey and Fowler

D. J. Harvey and J. R. Fowler, of Diamond Shamrock Corporation published a study performed on a quadruple effect chlorine-caustic evaporator.[2] A schematic of the evaporator is shown in Figure 2. The original control scheme consisted of proportional plus integral (PI) level control on the feed, PI level control on the primary vessel steam flow, PI secondary vessel level control on the primary vessel bottoms flow, and proportional plus integral plus derivative (PID) product composition control on the secondary vessel bottoms flow (product flow).

Momentum, heat, and mass balances were incorporated into a mathematical model of the evaporator. The Bernoulli equation was used to describe flow, with friction losses being described by the definition of the friction factor. Electrical flow analogies were used so that Kirchoff's Law could be applied to find all flow rates throughout the system. Experimentally determined pump curves were solved simultaneously with Bernoulli's equation by a trial-and-error process. For situations where flashing might take place due

to pressure drops, an approximation between incompressible and critical flows was employed. Corporate data were used for physical property calculations. Fourth-order Runge-Kutta integration was used throughout the model.

The first result of the simulation was that several pump impellers were found to be improperly sized, so that situation was corrected first. Disturbance inputs were evaluated as to their effects, and the seriousness of those effects. Feed locations were determined, and controller modes were selected. Unsteady-state operations, such as startup, shutdown, and fly-washing were also studied.

Chen, Carter, Miller, and Wheaton

Investigators at the University of Florida reported that computer control of a simulated three-effect, four-stage citrus juice evaporator yielded energy savings of 17%.[3] Product yield was improved, also, as burning of the juice (which results in downtime for cleaning of equipment, as well as discarded product) was avoided.

Kleinpeter and Weaver

J. A. Kleinpeter and R. E. C. Weaver, both of Tulane University, present a model of the flash separator shown in Figure 3, along with a recommended control strategy.[4,5] The model is quite involved, as it incorporates the Whitman Film Theory along with mass and energy balances. Ideal behavior of liquids and vapors was assumed, as was perfect mixing. Equations of state were used for densities, fugacities, and enthalpies. A fourth-order Runge-Kutta numerical integration was used to solve the resulting equations.

The model was then rewritten in linearized form, retaining only the first-order terms in the Taylor series expansion of each nonlinearity. LaPlace transformation of the resulting linear equations was undertaken, and the model then yielded a vector-matrix equation, namely

$$s * y(s) = A * x(s) + B * y(s)$$

where x(s) represents both control inputs and disturbance inputs, y(s) represents all state variables, and A and B are constants.

The controller was formed as

$$x(s) = F_1 * x(s) + F_2 * D(s) + F_3 * y(s) + F_4 * C(s) + F_4 * R(s)$$

where x(s) represents the manipulated inputs, D(s) represents the disturbance inputs, y(s) represents the controlled state variables, C(s) represents all other state variables, R(s) represents the setpoint vector, F_1 decouples the manipulated inputs, F_2 is a feedforward term to compensate for the disturbance inputs, F_3 decouples the noncontrolled state variables from the controlled state variables, and F_4 decouples the controlled state variables. It is noted that the resulting controller incorporates no dynamic elements.

The proposed controller was then compared for level, pressure, and temperature control against Ziegler-Nichols tuned PID controllers. It was found that for disturbance tuning, the PID controllers performed almost as well as the structural analysis control. However, when compared for set point changes, or servo control, the PID controllers produced considerable disturbances in the nonmonitored state variables, although they did control the control state variables well.

When structural analysis was attempted for composition control, it was found that the matrix A was singular, due to implicit coupling. The time domain description was utilized, and a similar procedure was performed to develop a control strategy. It was found that best control was obtained by deleting F_3 from the controller. Good disturbance control was available, but the servo control performance was not as good as that of the multiloop controller.

Newell, Fisher, and Seborg

R. B. Newell, D. G. Fisher, and D. E. Seborg, all of the University of Alberta, have published a series of papers on modeling of a double-effect evaporator and subsequent control studies.[6,7,8] Each effect was subdivided into five subsystems; steam chest, heat transfer surface, solution holdup, vapor space, and heat capacity of the evaporator itself. Density and enthalpy balances were written for the steam chest and the vapor space. A lumped-parameter heat balance was used to describe the heat transfer surface, as well as the heat capacity of the equipment. Mass, solute, and energy balances were written for the solution holdup. Boiling dynamics were ignored, and vapor-liquid equilibrium was assumed. Physical properties were calculated using empirical relationships, and the flow equations for the entire system were written. CSMP was used to write the simulation.

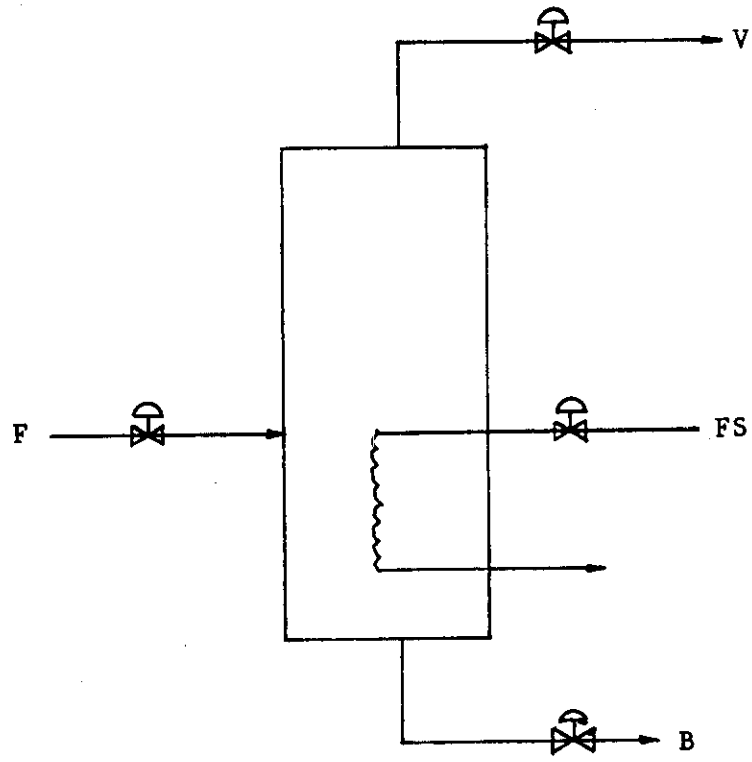

FIGURE 3. Flash Separator of Kleinpeter and Weaver

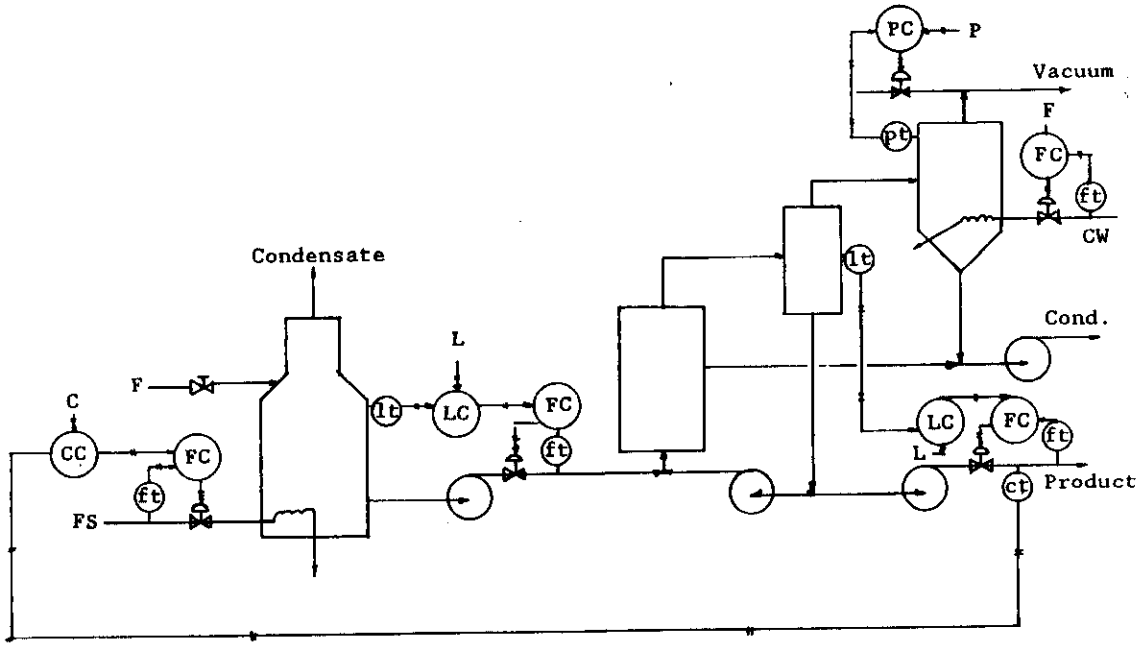

FIGURE 4. Evaporator at University of Alberta

The resulting tenth-order nonlinear model (10NL) was then linearized numerically, yielding a tenth-order linear model (10L) of the form

$$x = A * x + B * u$$

$$v = C * x$$

Some of the faster relationships were made steady-state to yield two additional models, 5NL and 5L. Further reductions were undertaken, resulting in three more models, 3LR, 3LD, and 2LD. It was found that the lower-order models not only deviated from experimental data in their dynamic behavior, but that they also exhibited significant steady-state offset. However, the lower-order models might find application for cases where the neglected relationships are unimportant. For example, liquid holdup might not be an important consideration if an additional level control system is applied to the evaporator.

Conventional multiloop control, predictive control, feedforward control, and optimal multivariable feedback control were evaluated with the multivariable control performing best and the multiloop control giving the poorest control. The other two methods fell in the order presented above.

The multiloop control system utilized product composition control on the feed, and cascaded level-flow loops on both evaporator vessels as shown in Figure 4. The feedforward control system utilized a control law of the form

$$u(iT) = K_{fb} * x(iT) + K_{ff} * d(iT)$$

where u represents the control vector, K_{fb} represents the feedback control matrix, K_{ff} represents the feedforward control matrix, x represents the state vector, d represents the load vector, and iT represents the particular point in time.

The multivariable controller took the form

$$u(iT) = K_{fb} * x(iT) + K_m * y_m(iT) + K_{sp} * y_{sp}(iT) + K_{ff} * d(iT)$$

where K_m represents a matrix of constants, y_m represents the model results, K_{sp} represents a matrix of constants, and y_{sp} represents the setpoint.

DESCRIPTION OF EVAPORATOR

The continuous evaporator is a thermosiphon type evaporator with an outboard reboiler. Feed is controlled by a Hackman Hat flow controller. The evaporator is shown in Figure 5 and the Hackman Hat is shown in Figure 6. The hat is simply a baffled vessel with an orifice at its bottom. Flow into the hat is under level control. With a constant level in the vessel, there is a constant flow into the evaporator from the hat. Feed from the hat enters the evaporator at the bottom of the reboiler. The liquid flows up through the tube side of the reboiler, through a large duct to the de-entrainment column. A smaller duct connects the de-entrainment column to the bottom of the reboiler.

Liquid exits the evaporator by gravity flow through a weir on the side of the de-entrainment column. Vapor flows up through a demisting tray into the condenser. The two demisting trays are dry bubble cap trays that drain through a downcomer into the column. The scrubbing tray is a bubble cap tray that maintains an inch of water for scrubbing entrained particulates from the vapor stream, and also drains through a downcomer into the column.

The vapor flows up through the center of the condenser and down through the tube side. The resulting liquid flows out by gravity flow. The liquid line is connected to the process vent, which is maintained at approximately one inch of water below atmospheric pressure. An overflow line is provided beyond the vent connection.

The evaporator is intended to concentrate uranyl nitrate solutions for further processing. Since a large percentage of steam use at SRP is in evaporation and Du Pont experience is that advanced control techniques can typically save 10% on steam use, the evaporator is a logical candidate for this study. It was felt that the project would be worthwhile for the knowledge gained about the process. Also, the controller now on the evaporator performs poorly, exhibiting oscillatory behavior.

MODEL DEVELOPMENT

Since the evaporator is production equipment on a tight schedule, it is unavailable for testing. Therefore the construction of a rigorous mathematical model was necessary. The bases of the model are differential mass and energy balances.

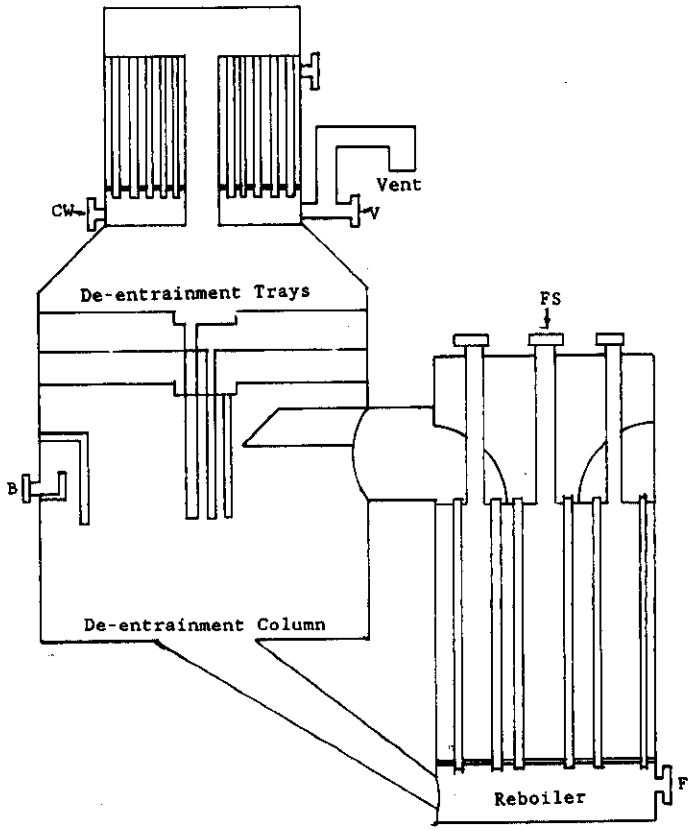

FIGURE 5. Continuous Evaporator at SRP

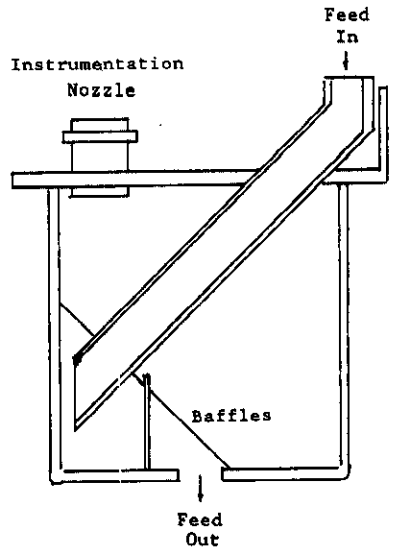

FIGURE 6. Continuous Evaporator Feed Connection (Hackman Hat)

Mass Balance

The mass balance was formulated as

$$F - B - V = dM/dt$$

where F is the feed flow rate, expressed in lb/hr, B is the bottoms flow rate, expressed in lb/hr, V is the vapor flow rate, expressed in lb/hr, and M is the mass of the solution in the evaporator, expressed in lb.

Perfect mixing was assumed for the liquid in the evaporator for use in composition calculations. This is a good assumption because the thermosiphon action between the de-entrainment column and the reboiler vessel provides excellent mixing.

Energy Balance

The energy balance was written in the following form:

$$F * T_f * CP_f + F_s * \lambda_s - V * \lambda_v - B * T * Cp = M * Cp * dT/dt$$

where T_f is the feed temperature, expressed in degrees fahrenheit, Cp_f is the heat capacity of the feed, expressed in BTU/lb/°F, F is the steam rate, expressed in lb/hr, λ_s is the latent heat of vaporization of the steam, expressed in BTU/lb, T is the temperature of the liquid in the evaporator, expressed in degrees fahrenheit, and Cp is the heat capacity of the liquid in the evaporator.

Vapor-Liquid Equilibrium

The vapor-liquid equilibrium was calculated using equations developed for the $Mg(NO_3)_2 - HNO_3 - H_2O$ system by Thompson, Derby, Stalzer, Counce, Jubin, and Barker.[9] They investigated three potential models: a full dissociation model, a simplified model, and a pseudobinary model. It was determined that the simplified dissociation model gave best agreement with experimental data. Therefore, the evaporator model included the simplified dissociation model. While it is true that the evaporator is used for the $UO_2(NO_3)_2 - HNO_3 - H_2O$ system, this model is the best available and should serve satisfactorily.

Dissociation

The simplified dissociation model predicts that the nitric acid will not fully dissociate, and expresses the equilibrium as

$$Ka = (X'_{a+} * x'_{-})/x'_{a}$$

where X'_{a+} is the mole fraction of the hydrogen ion, X'_{-} is the mole fraction of the nitrate ion, and X'_{a} is the mole fraction of the undissociated nitric acid. This approximation is valid at low acid concentrations, which fits the evaporator well. The equilibrium constant is expressed as

$$Ka = A \exp(-dH/R * T)$$

where A is a constant, dH is the heat of reaction, R is the gas constant, and T is the temperature in degrees centigrade. The mole fractions of the individual species can be expressed as a function of the analytical mole fractions and the extent of dissociation of the acid, α. It is assumed that the salt is totally dissociated, giving

$$X'_{a+} = (\alpha * X)/(1 + \alpha * X + 2 * X)$$

$$X'_{-} = (\alpha * X + 2 * X)/(1 + \alpha * X + 2 * X)$$

$$X'_{a} = (1 - \alpha) * X/(1 + \alpha * X + 2 * X)$$

$$X'_{w} = X/(1 + \alpha * X + 2 * X)$$

where the w refers to water and the unprimed X's refer to the analytical mole fraction, or the number of moles of the compound present in the solution. By substitution of these equations into the simplified equilibrium expression we get

$$Ka = (2 * \alpha * X_a + 2 * \alpha * X_s)/(1 + \alpha * X_a + 2 * X_s)(1 - \alpha)$$

Vapor Pressures

Given the analytical mole fractions and the temperature, the dissociated mole fractions can be calculated. The following Antoine equations were then used to find the equilibrium vapor pressures of water and acid:

$$\log_{10} P_w = 7.949 - 1657.4/(T + 227.1)$$

$$\log_{10} P_a = 7.616 - 1486.2/(T + 230.0)$$

where T is expressed in degrees centigrade, P_a is the equilibrium vapor pressure of the acid, and P_w is the equilibrium vapor pressure of the water.

Activity Coefficients

Next, the activity coefficients were calculated. Assuming the effect of pressure to be negligible, the natural logarithms of the activity coefficients can be approximated by a second order polynomial expression in X_a and X_s as

$$\ln \gamma'_a = -2.52 + 6.21 X_a - 3.10 X_a^2 + 23.83 X_s$$

$$- 24.20 X_s^2 - 15.8 X_a * X_s$$

$$\ln \gamma'_w = -0.17 X_a - 3.62 X_a^2 - 4.47 X_s - 15.83 X_s^2$$

$$- 28.20 X_a * X_s$$

Total Pressure

The total pressure at the liquid surface in the evaporator can then be expressed as

$$Pt = \gamma'_a * X'_a * P_a + \gamma'_w * X'_w * P_w$$

Vapor Flow

The valve equation is then used to relate vapor flow to the pressure differential between the pressure at the liquid surface as found from the vapor-liquid equilibrium and the pressure at the top as maintained by the process vent:

$$V = 9185.0 \sqrt{(P_e - P_c)}$$

where P_e is the pressure at the liquid surface, expressed in inches of water pressure, and P_c is the pressure in the condenser, also expressed in inches of water pressure.

Specific Gravity

The specific gravity was calculated from an equation obtained at SRP:

$$0.001345\ C = \rho - 1.0042 + 0.000001(8.4\ \rho - 2.4)T^2$$

$$- 0.01(0.00314\ C + 2.51)Na$$

where T is the temperature expressed in degrees centigrade, ρ is the specific gravity of the solution expressed in g/mL, C is the uranium concentration expressed in g/L, and Na is the normality of the acid in the solution.

Cooling Water Temperature

The exit temperature of the cooling water was calculated from an energy balance assuming total condensation, which operating practice indicates is the case, as the exit temperature of the cooling water is kept at or below 50 degrees centigrade.

Temperature

The energy balance was implemented in the z-transform form in order to promote stability:

$$T = T \exp(-dt/\tau) + \left(1 - \exp(-dt/\tau)(F * T_f * Cp_f/B * Cp)\right.$$

$$\left. - (V * \lambda_v/B * Cp) + (F_s * \lambda_s/B * Cp)\right)$$

where $\tau = M/B$.

Bottoms Flow

The bottoms flow was determined using the valve equation to relate the liquid height in the weir to flow:

$$B = K\sqrt{(H - HO)}$$

where K is the valve constant, H is the liquid height in the evaporator, expressed in inches, and HO is the height of the weir above the bottom of the evaporator, also expressed in inches.

Implementation

The model was implemented on a Digital Equipment Corp. DOP-10 computer using a step time of one second. The major inputs were identified as feed flow, steam flow, feed composition, feed temperature, and vent pressure. The possible control variables were identified as being pressure, temperature, specific gravity, liquid height, vapor flow, and bottoms flow. The effect of each input on each output was observed and graphed by computer.

Effect of Vent Pressure Disturbance

It was found that the effect of a vent pressure disturbance could be neglected, as the initial effect was minimal, and the system quickly returned almost to the undisturbed condition, as can be seen from the effect on the vapor flow rate of a decrease of one inch of water pressure in the condenser in Figure 7.

Effect of Feed Flow Disturbance

The effect of a feed increase on the specific gravity can be seen in Figure 8. The temperature shows an initial rise because the feed is an important contributor to the heat balance, followed by a pseudo-first-order decrease, as shown in Figure 9.

The pressure shows the same initial increase, followed by a large decrease due to the decreased heat/feed ratio. This is followed by a slow pseudo-first-order increase, as shown in Figure 10. The increase is caused by the increase in nitric acid concentration and the decrease in the salt concentration. The vapor rate, as shown in Figure 11, naturally follows the pressure.

The liquid height shows an immediate rise followed by a pseudo-first-order decrease due to the vapor rate increase, as shown in Figure 12. The bottoms flow follows the liquid height, as shown in Figure 13.

Effect of Steam Flow Disturbance

The effect of a steam decrease is essentially the same as the effect of a feed increase, as can be seen from Figures 14, 15, 16, 17, 18, and 19.

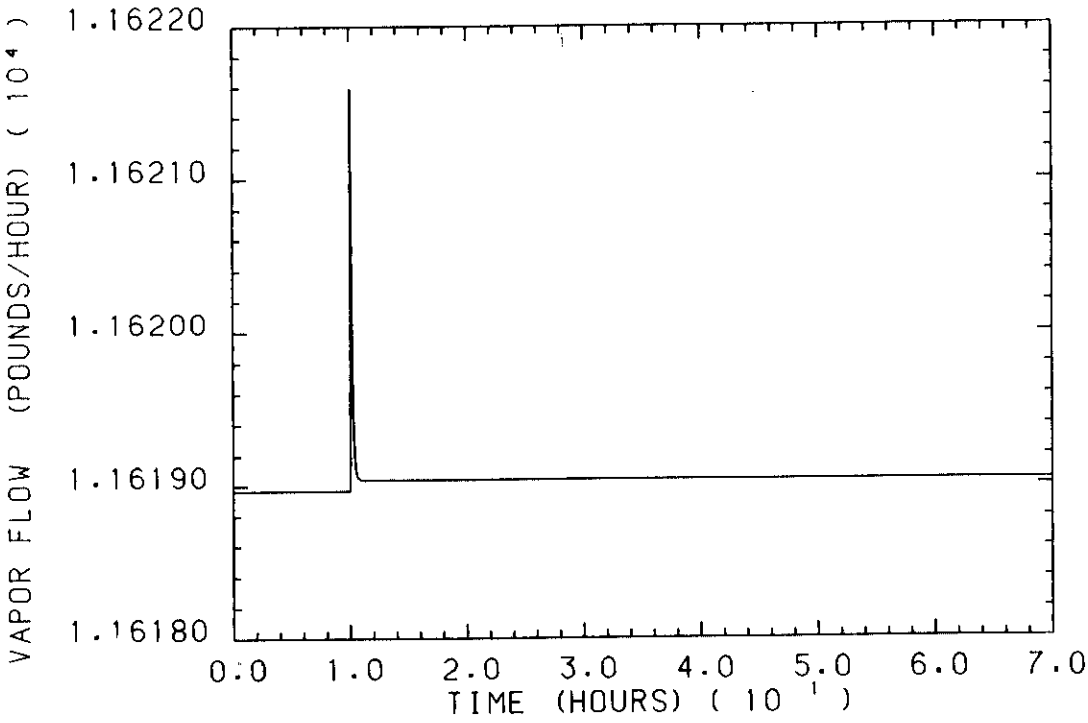

FIGURE 7. Effect of Vent Pressure Decrease on Vapor Flow

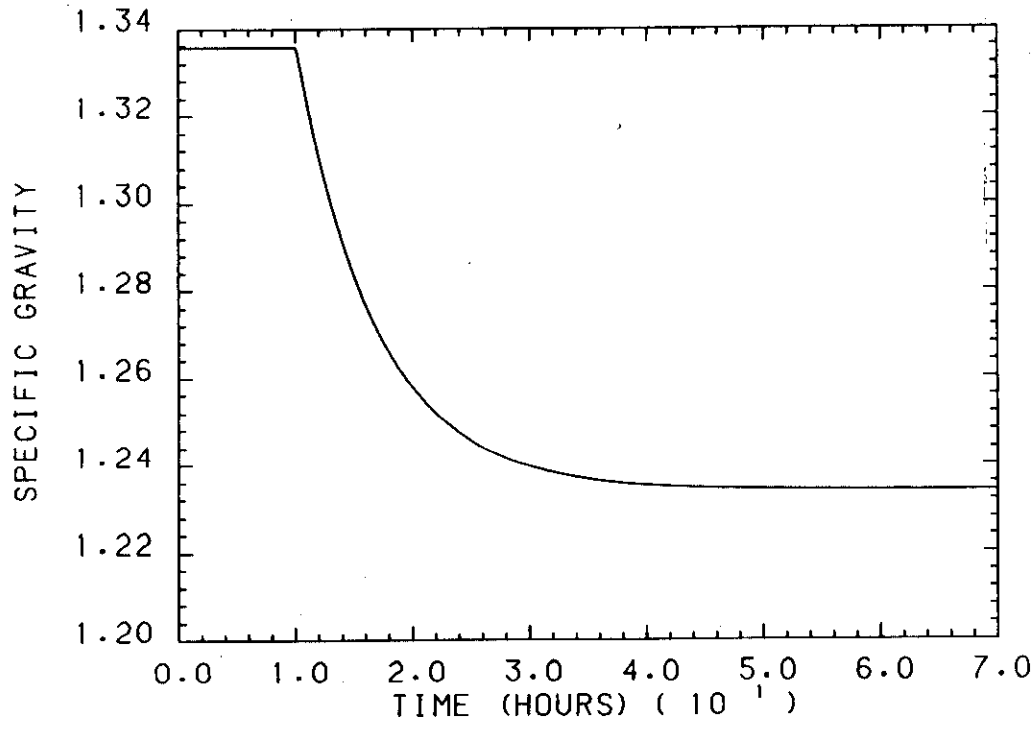

FIGURE 8. Effect of Feed Increase on Specific Gravity

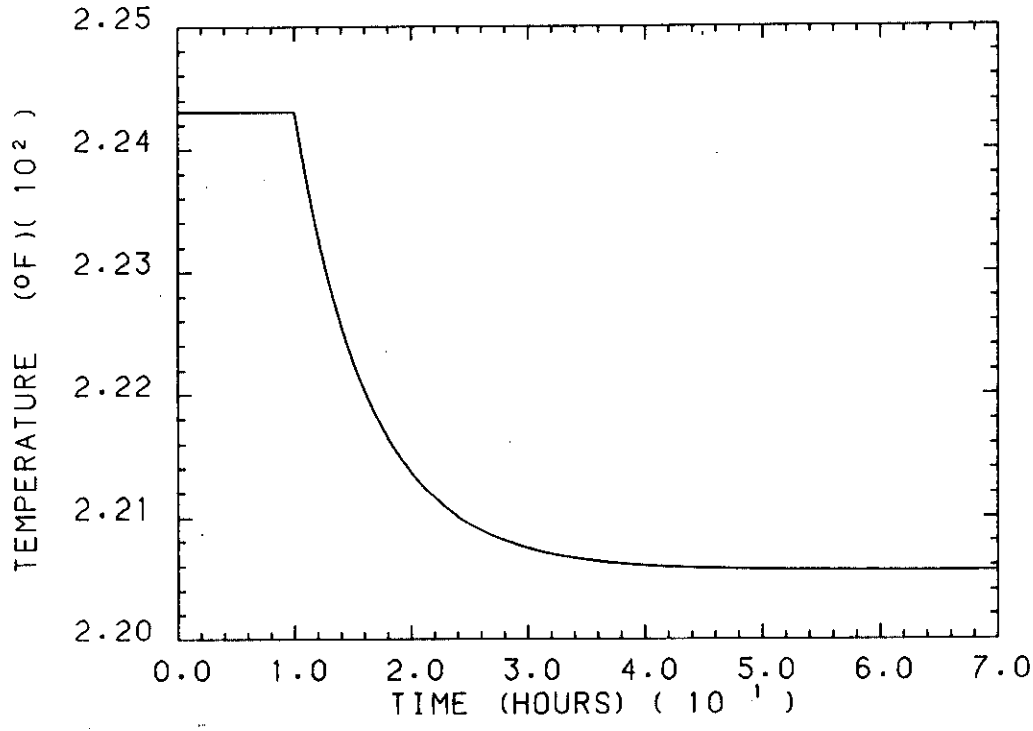

FIGURE 9. Effect of Feed Increase on Temperature

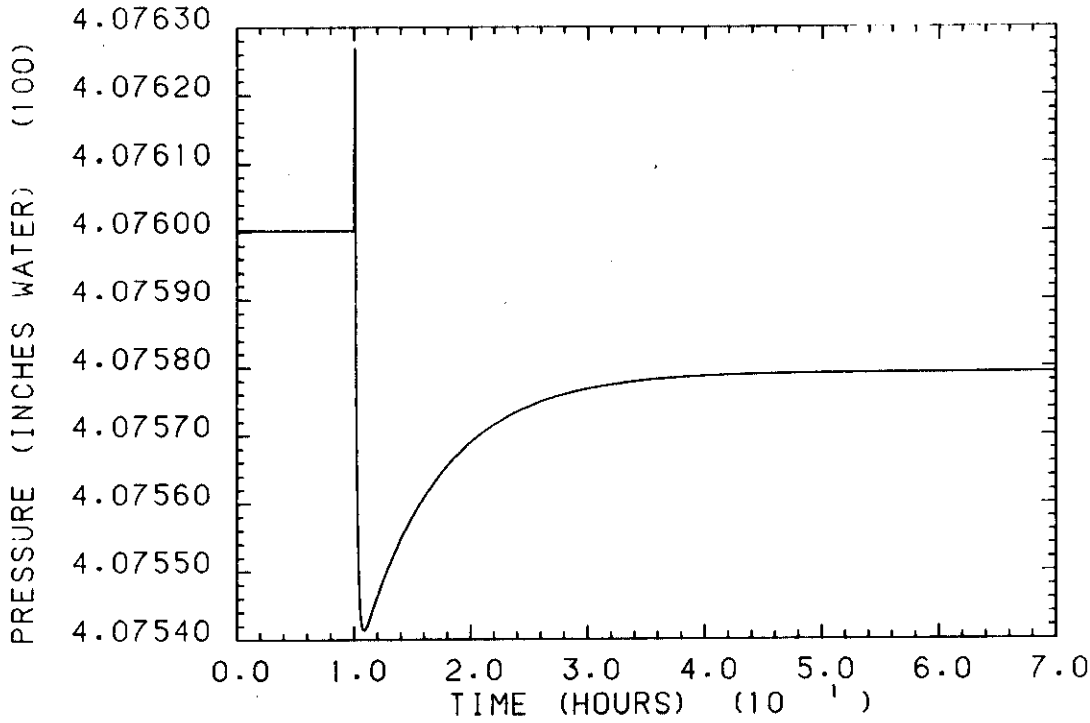

FIGURE 10. Effect of Feed Increase on Pressure

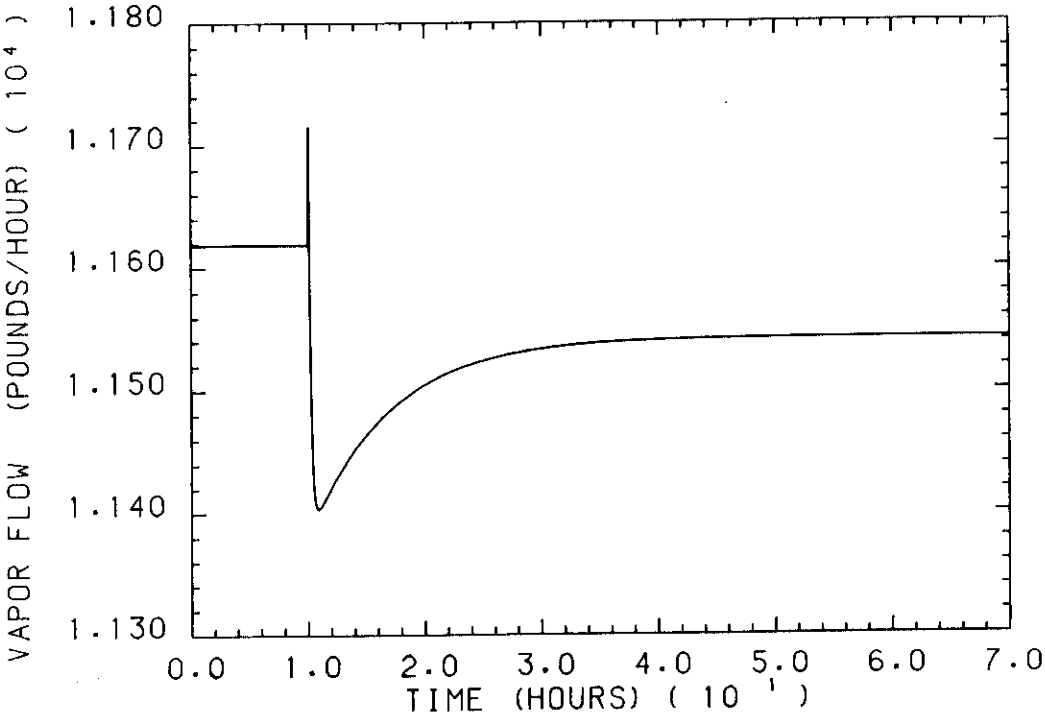

FIGURE 11. Effect of Feed Increase on Vapor Flow

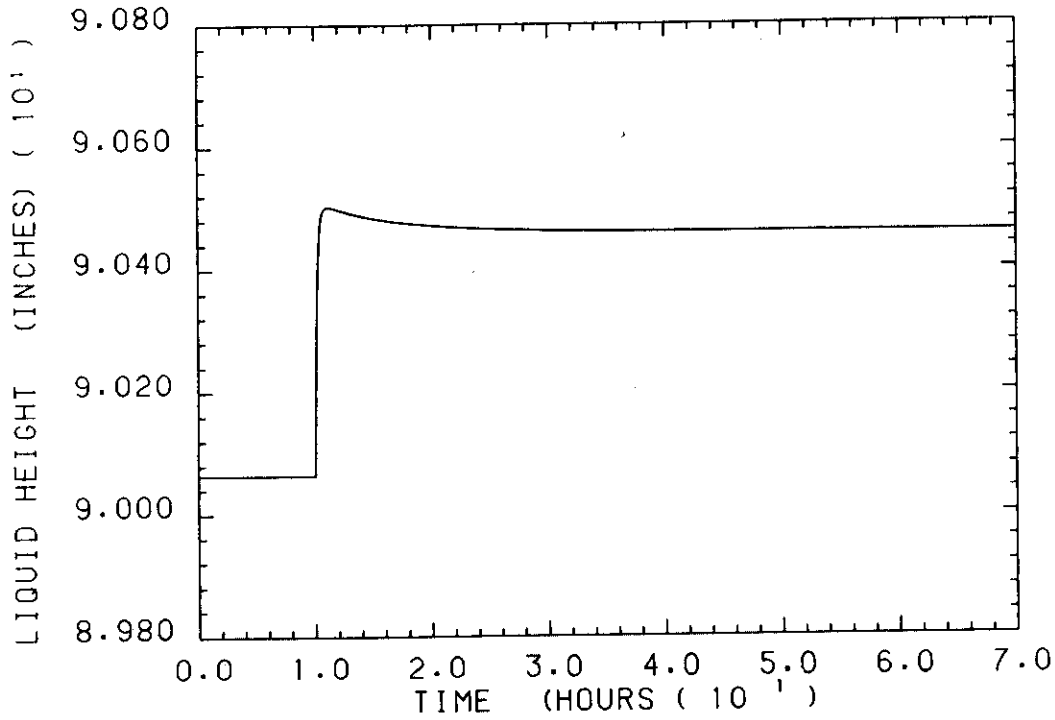

FIGURE 12. Effect of Feed Increase on Liquid Height

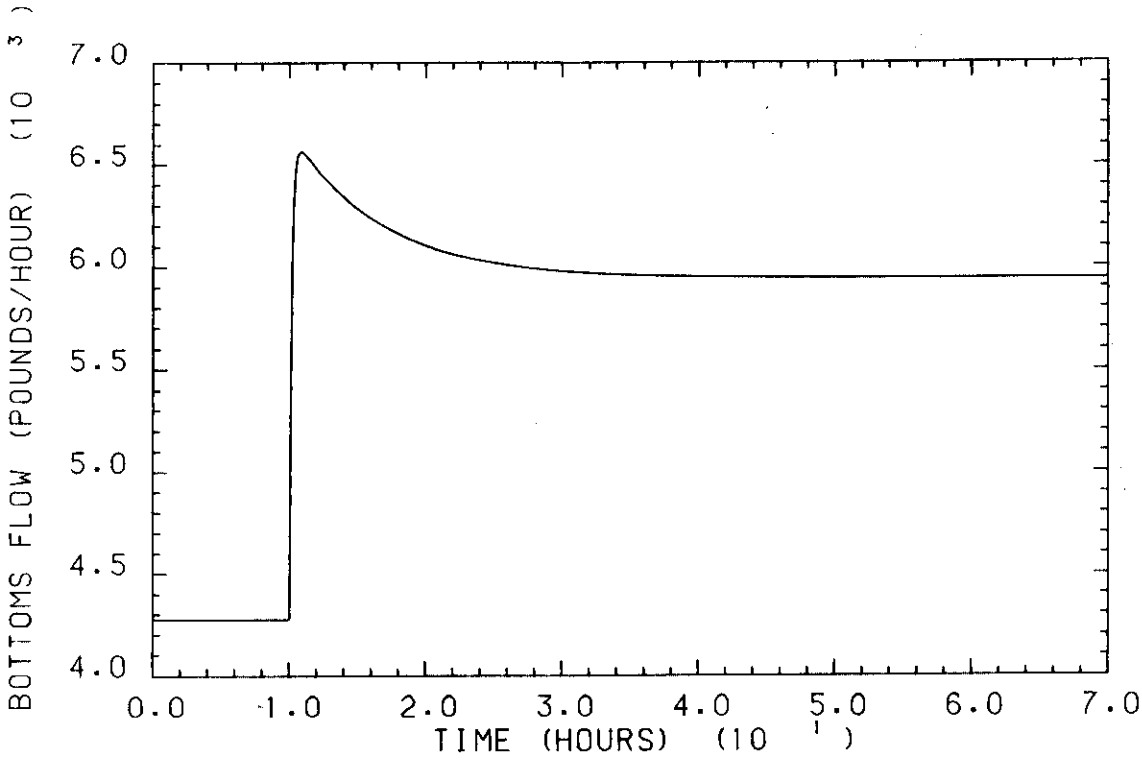

FIGURE 13. Effect of Feed Increase on Bottoms Flow

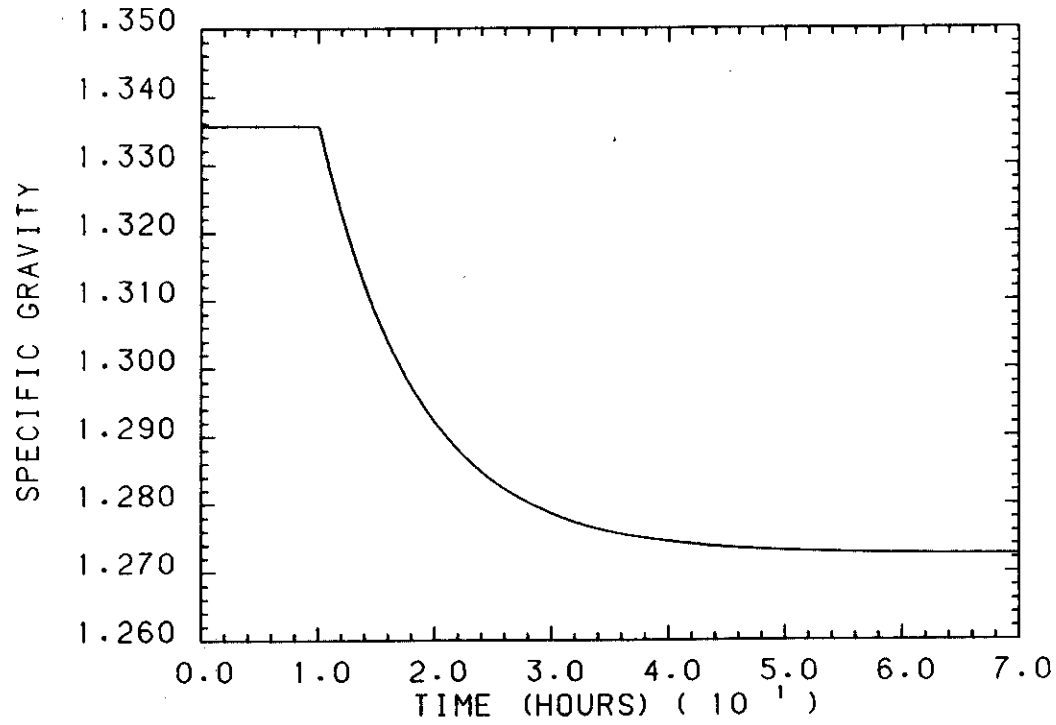

FIGURE 14. Effect of Steam Decrease on Specific Gravity

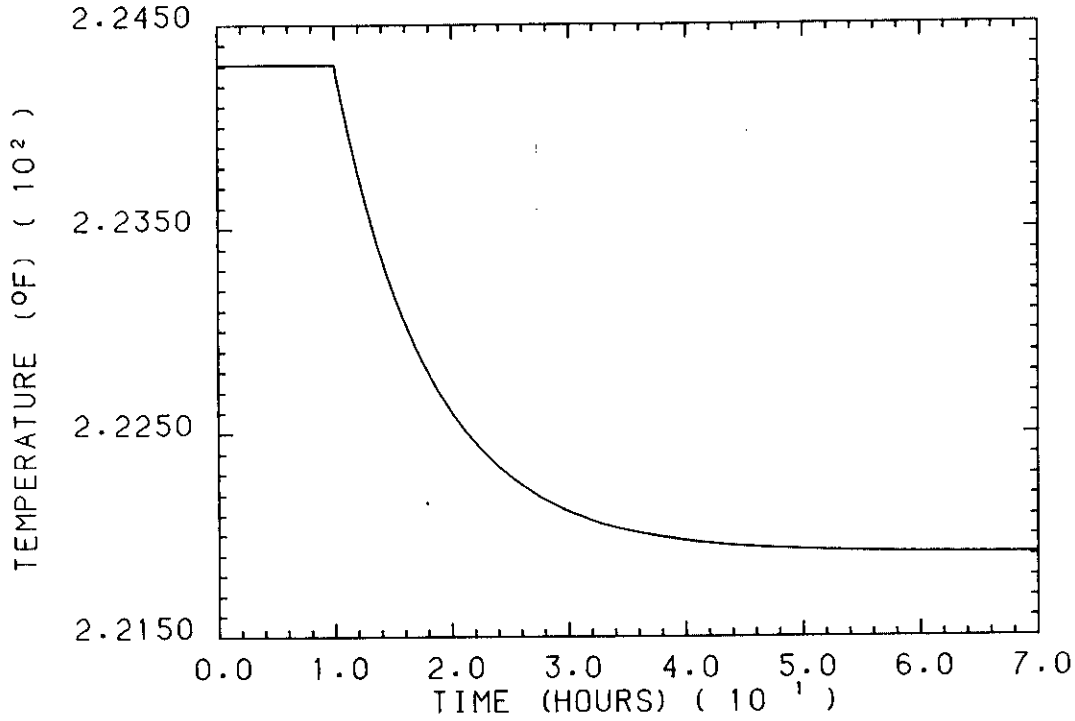

FIGURE 15. Effect of Steam Decrease on Temperature

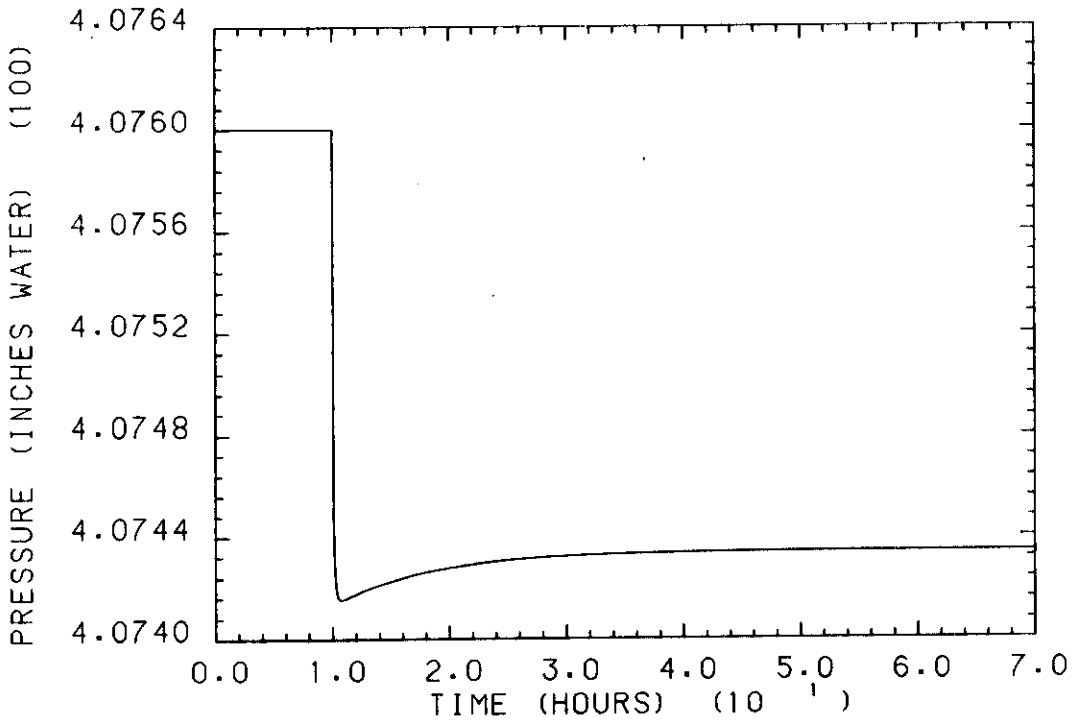

FIGURE 16. Effect of Steam Decrease on Pressure

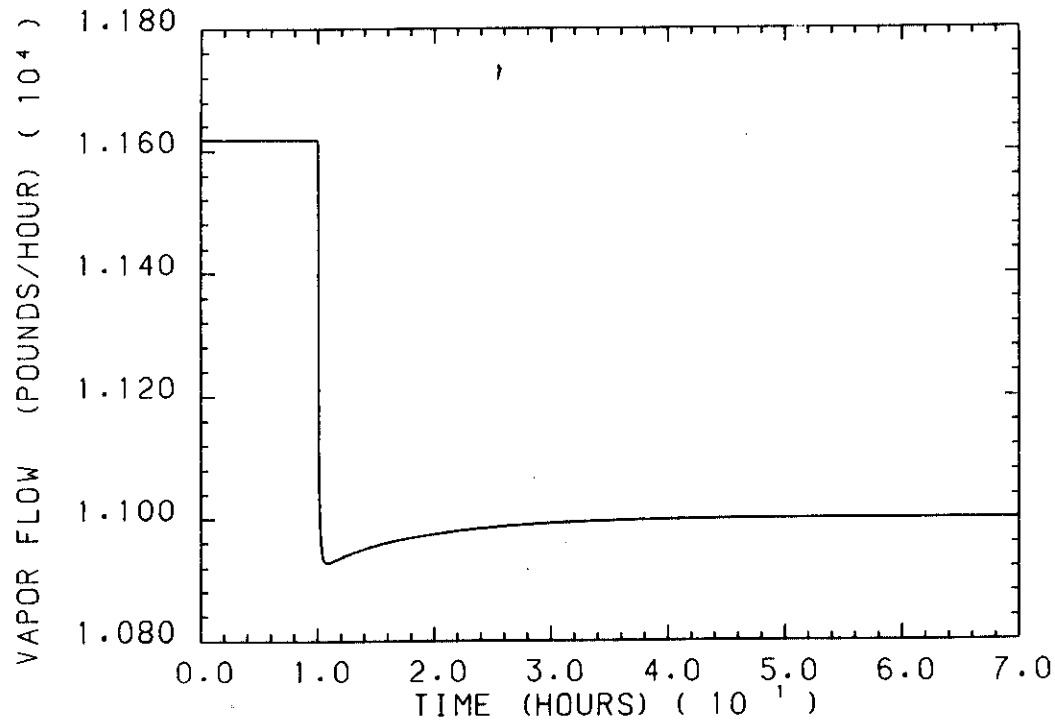

FIGURE 17. Effect of Steam Decrease on Vapor Flow

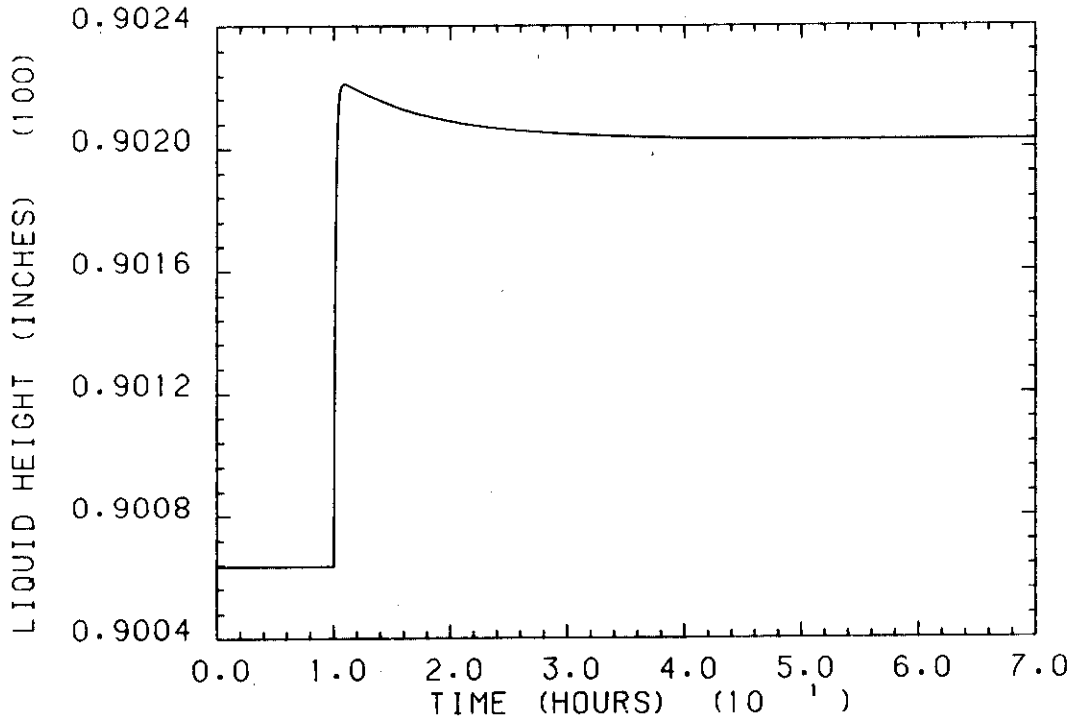

FIGURE 18. Effect of Steam Decrease on Liquid Height

Effect of Feed Temperature Disturbance

The effect of a feed temperature increase is analogous to the effect of a steam increase, as can be seen from Figures 20, 21, 22, 23, 24, and 25.

Effect of Feed Composition Disturbance

The effect of a feed acid increase is minimal, as can be seen from the effect of a 90% increase in feed acid on the temperature in Figure 26, and on pressure, in Figure 27.

The effect of a feed salt increase could be quite serious, as can be seen from Figure 28, the effect on specific gravity of a 90% increase in feed salt concentration. In this example, when the salt concentration in the feed is increased from 10.5 wt % to 20 wt %, the specific gravity of the solution in the evaporator rises from 1.32 to 1.86. Fortunately, the pH of the incoming solution is well maintained by the equipment upstream of the evaporator.

LINEARIZED MODEL

Since the complete evaporator model contains both very fast and very slow dynamic elements, namely vapor flow, which responds very quickly, and specific gravity, which responds very slowly, the resulting simulation was extremely stiff. To minimize the extremely large computational requirements, a model was developed based on relatively simple linear transfer function relationships. The simplified model was developed by collecting step response data on the full model and curve fitting the parameters of a series of first order lags with dead times. Up to three elements were used to describe each relationship.

A good example is the response of vapor flow to a feed flow disturbance, as was shown in Figure 10. The relationship was described as a sum of three transfer functions as shown below:

$$V(s)/F(s) = K_1 * \exp\left(-\Theta_1(s)\right)/\left(1 + \tau_1(s)\right) + K_2 * \exp\left(-\Theta_2(s)\right)/\left(1 + \tau_2(s)\right) + K_3 * \exp\left(-\Theta_3(s)\right)/\left(1 + \tau_3(s)\right)$$

where V(s) is the vapor rate, expressed in lb/hr, F(s) is the feed rate, expressed in lb/hr, K is a steady-state gain, τ is a time constant, expressed in hours, and Θ is a dead time, expressed in hours. The steady-state gains for each relationship were used and the time constants and dead times were fit by hand; they are found in Tables I through 6.

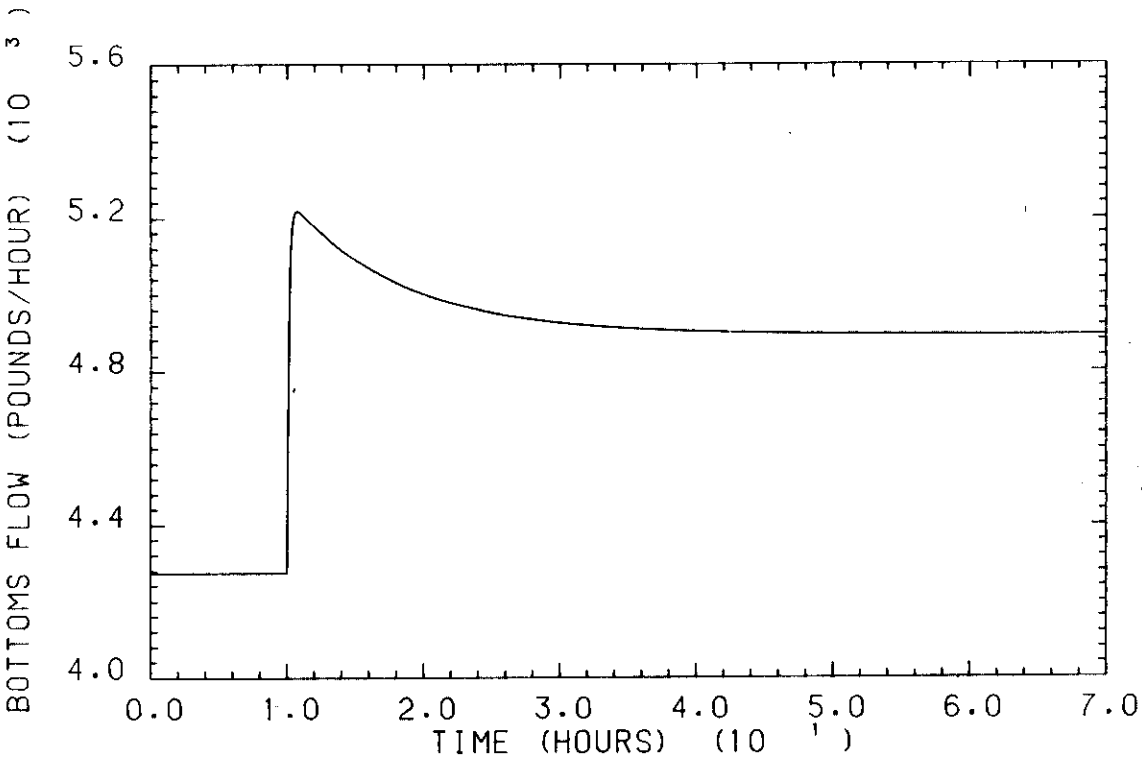

FIGURE 19. Effect of Steam Decrease on Bottoms Flow

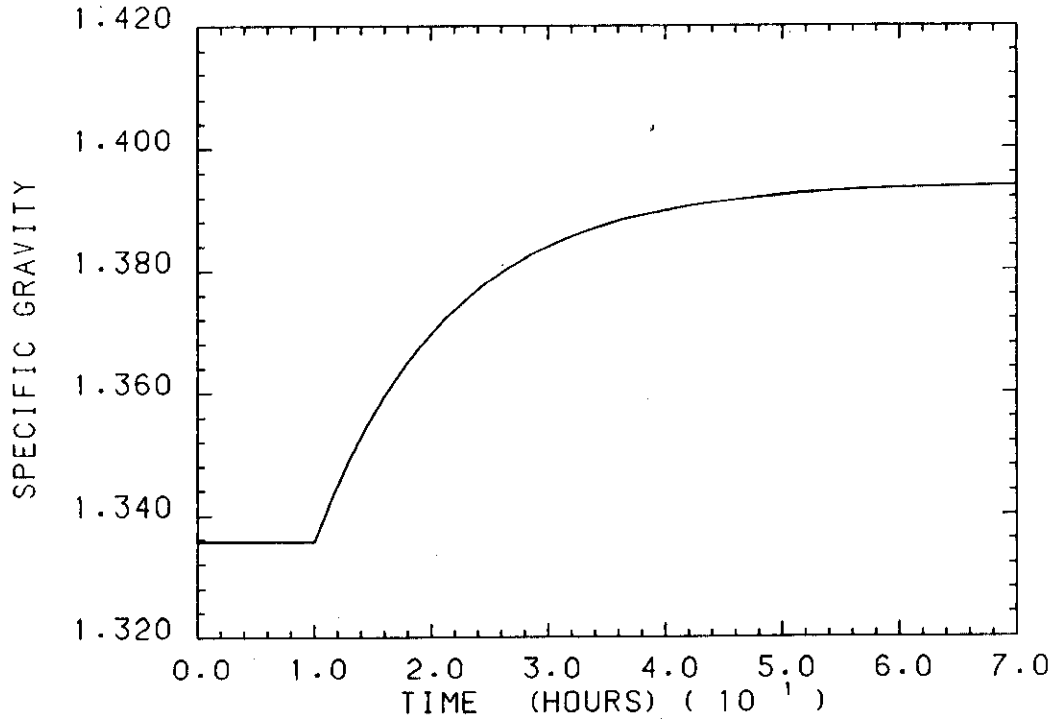

FIGURE 20. Effect of Feed Temperature Increase on Specific Gravity

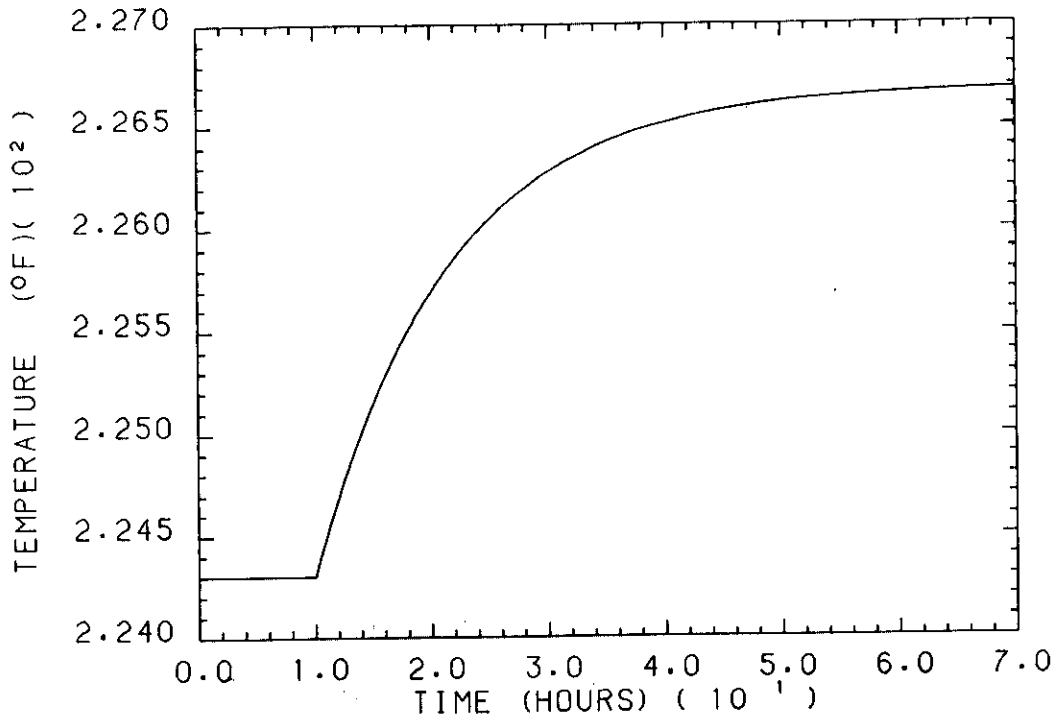

FIGURE 21. Effect of Feed Temperature Increase on Temperature

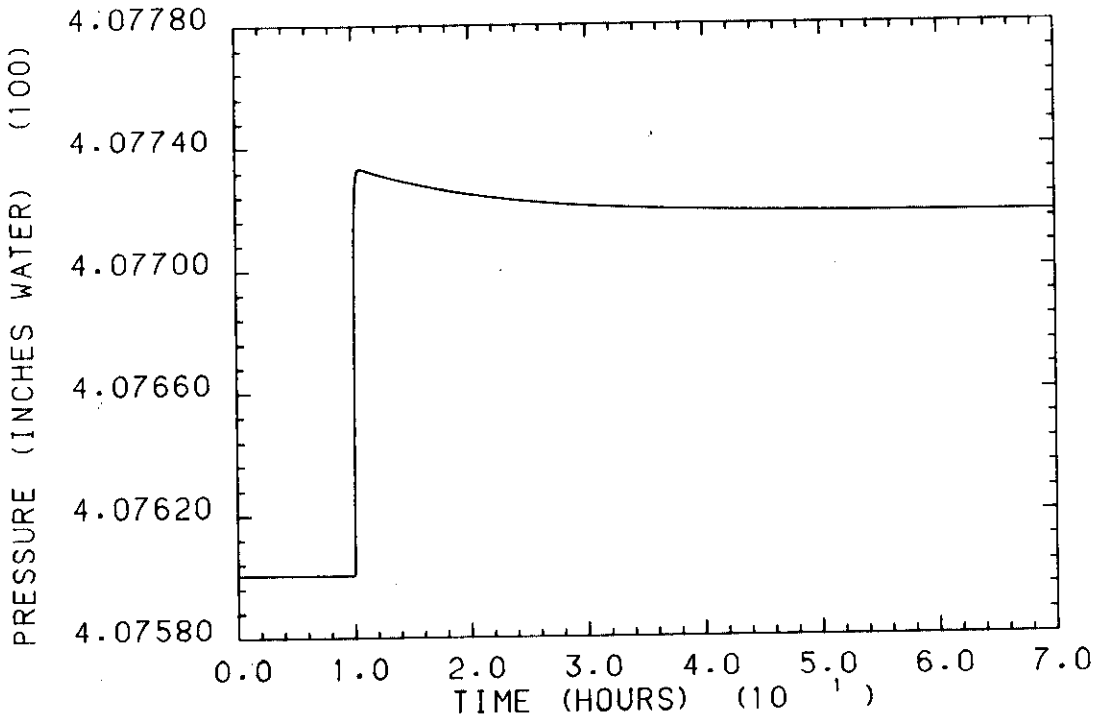

FIGURE 22. Effect of Feed Temperature Increase on Pressure

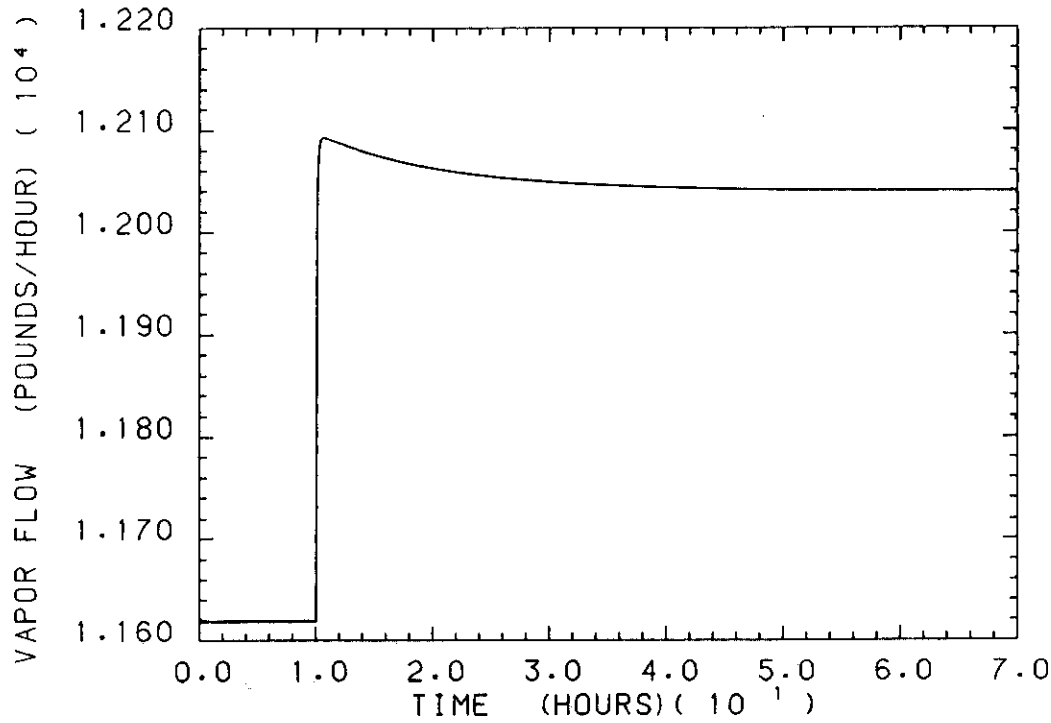

FIGURE 23. Effect of Feed Temperature Increase on Vapor Flow

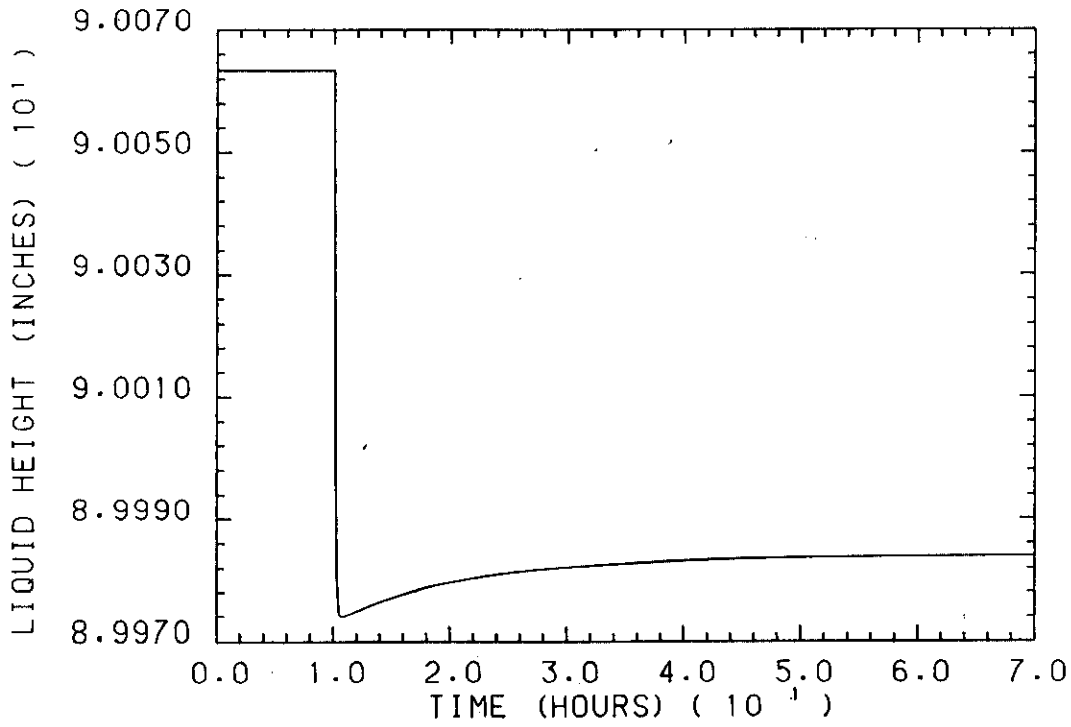

FIGURE 24. Effect of Feed Temperature Increase on Liquid Height

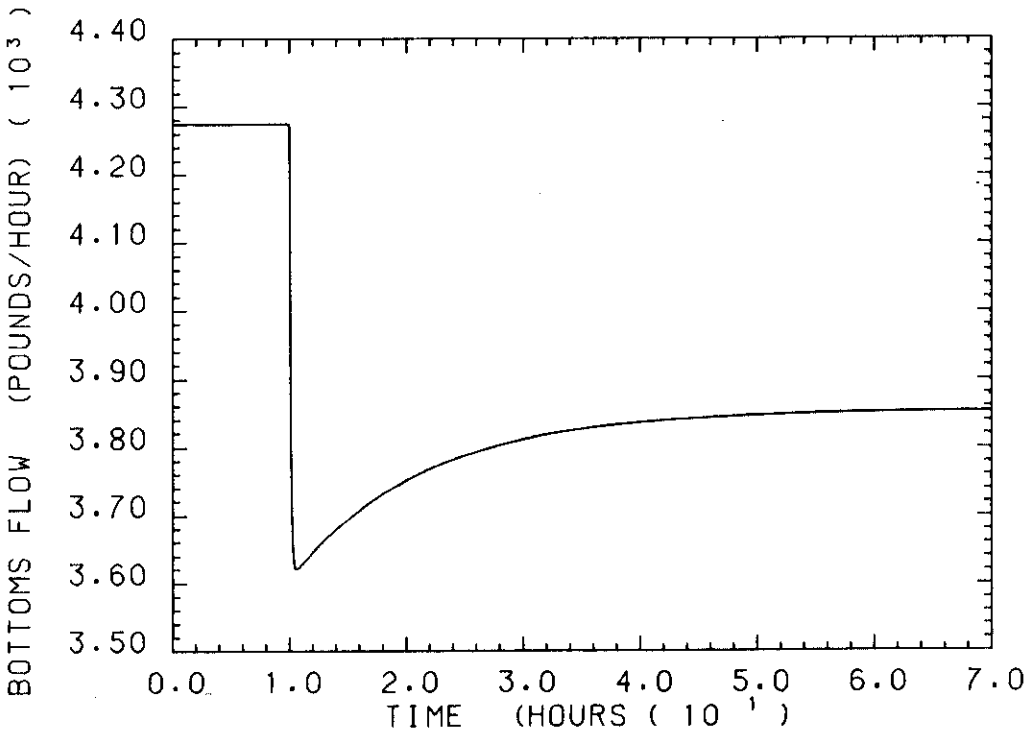

FIGURE 25. Effect of Feed Temperature Increase on Bottoms Flow

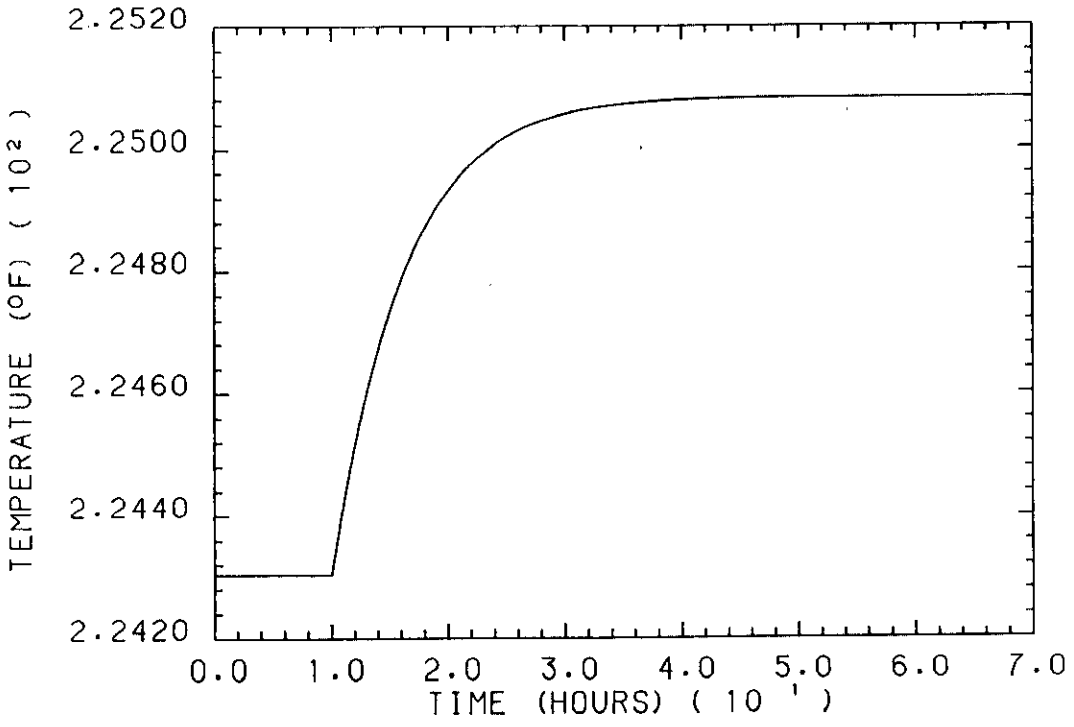

FIGURE 26. Effect of Feed Acid Increase on Temperature

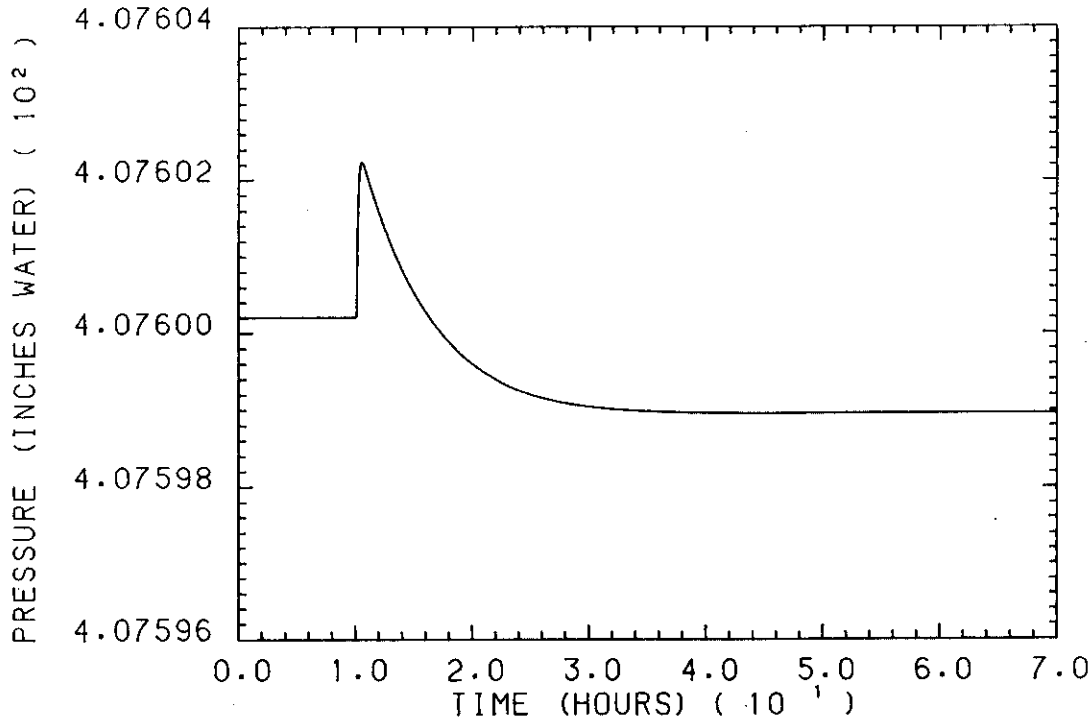

FIGURE 27. Effect of Feed Acid Increase on Pressure

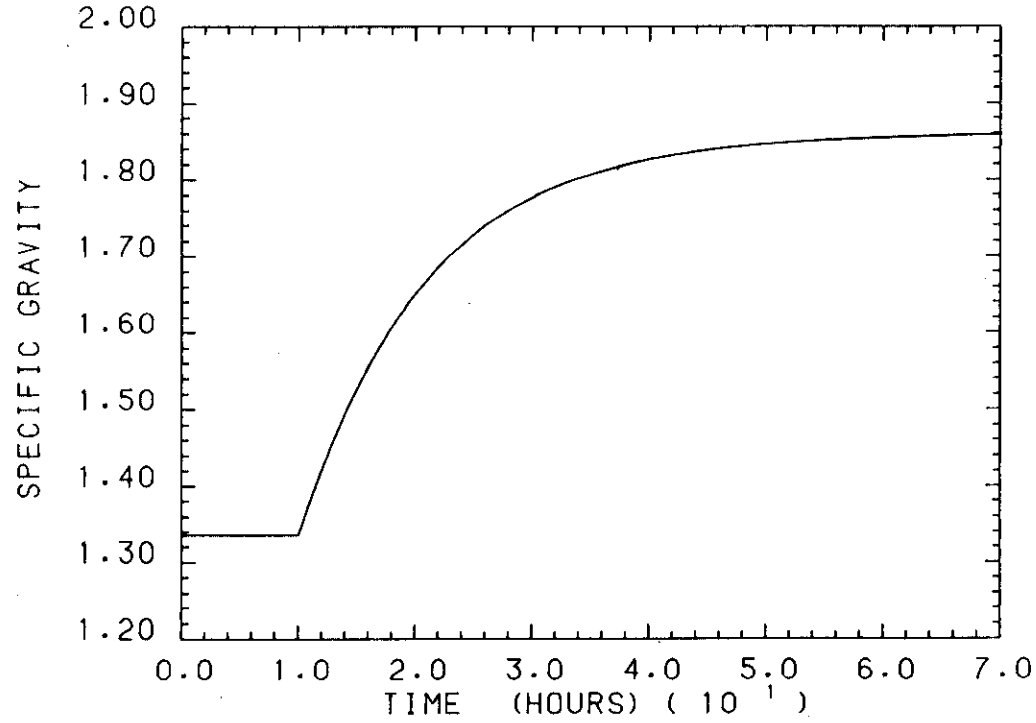

FIGURE 28. Effect of Feed Salt Increase on Specific Gravity

TABLE 1

Parameters for Linearized Model of Effect of Steam Disturbance

Output Variable	Gain	Time Constant	Dead Time
Specific Gravity	1.2615×10^{-4}	8.2200	-
Temperature	4.7915×10^{-4}	8.0000	-
Pressure I	3.6965×10^{-4}	0.0515	-
Pressure II	-3.8053×10^{-4}	8.5330	0.7330
Vapor Flow I	1.3832	0.1000	-
Vapor Flow II	-0.1464	8.5333	0.7333
Liquid Height I	-3.1537×10^{-4}	0.0860	-
Liquid Height II	3.7280×10^{-4}	8.5000	0.8667
Bottoms Flow I	-1.8898	0.0500	-
Bottoms Flow II	0.6525	8.4667	0.7333

TABLE 2

Parameters for Linearized Model of Effect of Feed Disturbance

Output Variable	Gain	Time Constant	Dead Time
Specific Gravity	-1.2187×10^{-4}	12.750	-
Temperature	-5.0820×10^{-4}	13.000	-
Pressure I	1.8027×10^{-5}	0.006	-
Pressure II	-8.1276×10^{-5}	0.060	-
Pressure III	4.3947×10^{-5}	13.270	0.6000
Vapor Rate I	0.0412	0.000	-
Vapor Rate II	-0.1850	0.100	-
Vapor Rate III	0.0997	12.660	0.6000
Liquid Height I	1.8832×10^{-4}	0.080	-
Liquid Height II	-1.6191×10^{-5}	13.260	0.8000
Bottoms Flow I	1.4788	0.000	-
Bottoms Flow II	-0.4311	13.260	-

TABLE 3

Parameters for Linearized Model of Effect of Feed Temperature Disturbance

Output Variable	Gain	Time Constant	Dead Time
Specific Gravity	2.9067×10^{-3}	11.300	-
Temperature	0.1188	13.000	-
Pressure I	6.6555×10^{-3}	0.060	-
Pressure II	-7.6052×10^{-4}	11.267	0.6000
Vapor Flow I	23.6800	0.060	-
Vapor Flow II	-2.6587	21.267	0.6000
Liquid Height I	-4.4761×10^{-3}	0.070	-
Liquid Height II	4.9699×10^{-4}	11.270	0.7333
Bottoms Flow I	$-3.2664 \times 10^{+1}$	0.070	-
Bottoms Flow II	11.5920	11.267	0.6000

TABLE 4

Parameters for Linearized Model of Effect of Vent Pressure Disturbance

Output Variable	Gain	Time Constant	Dead Time
Specific Gravity	-2.6955×10^{-4}	0.000	-
Temperature	0.1253	0.000	-
Pressure	0.9998	0.000	-
Vapor Flow I	$-2.6367 \times 10^{+1}$	0.000	-
Vapor Flow II	$2.5643 \times 10^{+1}$	0.080	-
Liquid Height I	1.6404×10^{-2}	0.000	-
Liquid Height II	-1.6174×10^{-2}	0.150	-
Bottoms Flow I	$1.1110 \times 10^{+2}$	0.000	-
Bottoms Flow II	$-1.1040 \times 10^{+2}$	0.100	-

TABLE 5

Parameters for Linearized Model of Effect of Feed Acid Concentration Disturbance

Output Variable	Gain	Time Constant	Dead Time
Specific Gravity	$3.5589 \times 10^{+1}$	1.000	-
Temperature I	$3.7718 \times 10^{+3}$	2.778	-
Temperature II	$-3.6450 \times 10^{+1}$	5.500	12.533
Pressure I	$1.6457 \times 10^{+1}$	0.000	-
Pressure II	$-2.2993 \times 10^{+1}$	1.200	-
Pressure III	0.4182	5.100	11.667
Vapor Flow I	$5.8997 \times 10^{+4}$	0.035	-
Vapor Flow II	$-8.2850 \times 10^{+4}$	1.200	0.333
Vapor Flow III	1.5332	4.500	11.200
Liquid Height I	$-5.0216 \times 10^{+1}$	0.030	-
Liquid Height II	$3.9418 \times 10^{+1}$	1.500	0.333
Bottoms Flow I	$-4.6816 \times 10^{+5}$	0.035	-
Bottoms Flow II	$4.9569 \times 10^{+5}$	1.200	0.333
Bottoms Flow III	$5.4010 \times 10^{+3}$	6.000	13.067

TABLE 6

Parameters for Linearized Model of Effect of Feed Salt Concentration Disturbance

Output Variable	Gain	Time Constant	Dead Time
Specific Gravity	0.0913	5.630	-
Temperature	8.1782	6.000	-
Pressure I	2.1396×10^{-2}	0.000	-
Pressure II	-3.4532×10^{-2}	6.467	-
Vapor Flow I	$7.7654 \times 10^{+1}$	0.060	-
Vapor Flow II	$-1.2535 \times 10^{+2}$	4.000	0.4667
Liquid Height I	-9.1994×10^{-2}	0.053	-
Liquid Height II	5.6490×10^{-2}	6.000	0.5333
Bottoms Flow I	$-6.0860 \times 10^{+2}$	0.060	-
Bottoms Flow II	$6.5643 \times 10^{+2}$	4.000	0.4667

In LaPlace form, the model can be described via a matrix. Thus, a disturbance in any or all of the inputs can be related to each output. This model was used for the control method selection and for preliminary tuning of the controller. This simplified model utilized difference equations to represent the process and was run with a step time of one minute.

The form of the difference equation is:

$$dX(i) = -a * X(i-1) + b * M(i-1-n)$$

$$X(i) = X_{ss} + \Sigma dX(i)$$

$$n = N/dt$$

$$alpha = \exp(-dt/T)$$

$$a = -alpha$$

$$b = K(1 - alpha)$$

where X(i) is the current value of the output, dX(i) is the effect on the output of the input, X_{ss} is the steady-state value of the output, M is the value of the input, N is the dead time, expressed in hours, n is the integer dead time, T is the time constant of the particular relation, expressed in hours, and a and b are the difference equation constants.

HACKMAN HAT FLOW CONTROLLER

In order to properly simulate the actual control system, the Hackman Hat flow control was simulated. The valve equation was used to relate liquid height in the hat to flow:

$$F = K_{hat}\sqrt{h}$$

where F is the feed into the evaporator, expressed in lb/hr, K_{hat} is the valve constant, and H is the liquid height in the hat, expressed in inches.

The hat has fairly quick response to a feed decrease, as can be seen in Figure 29, which compares the feed flow to the hat and the flow from the hat.

A proportional controller was added to the hat to control the liquid height in the hat using the feed to the hat. The proportional controller was chosen because it is the simplest type of controller and has the fastest and most stable response. The offset that accompanies the use of a proportional controller is of

no consequence in the inner loops of a control system, which is where the hat is used. The response of the tuned system is shown in Figure 30. The system was tuned for a quarter decay response.

CONTROL SYSTEMS

Present System

The first control system tested was the system that is presently used on the evaporator at SRP. The Hackman Hat flow control was coupled to the evaporator, and a PI controller was used as the master controller for the Hackman Hat liquid height control. A block diagram of the control system is shown in Figure 31. The PI controller was chosen in order to eliminate offset from the system. The Hackman Hat liquid level controller was detuned slightly, with the gain reduced from 760 to 660. The specific gravity controller was then tuned using a Pattern Search to minimize the integral time times absolute error (ITAE) plus a constant times the integral of the absolute derivative of the control action (CONAC).

$$ITAE = \int time * error(t) * dt$$

$$CONAC = \beta \int \left| d\ C(t)/dt \right| * dt$$

where error is the deviation of the control variable from the set-point, time is the elapsed time since the disturbance, expressed in hours, β is a tuning constant, and C(t) is the manipulated variable.

The Pattern Search utilizes a subroutine, PATERN,[11] which determines the values of parameters (the gain and integral time of the specific gravity controller) which minimize the COST (ITAE + CONAC). The constant was chosen as 0.006 which was the value which minimized the "ringing" behavior of the control system. The gain and integral time were chosen as -4117.25 and 0.1547 hours, respectively. The response of the system to a 20°F increase in feed temperature is shown in Figure 32. The control action is shown in Figure 33.

Steam Controller

The first alternate system that was considered used the steam flow, rather than the feed flow, as the manipulated variable. A block diagram is shown in Figure 34. The response of the system to the steam controller is almost identical to the response of the system to the feed controller. However, since the evaporator is

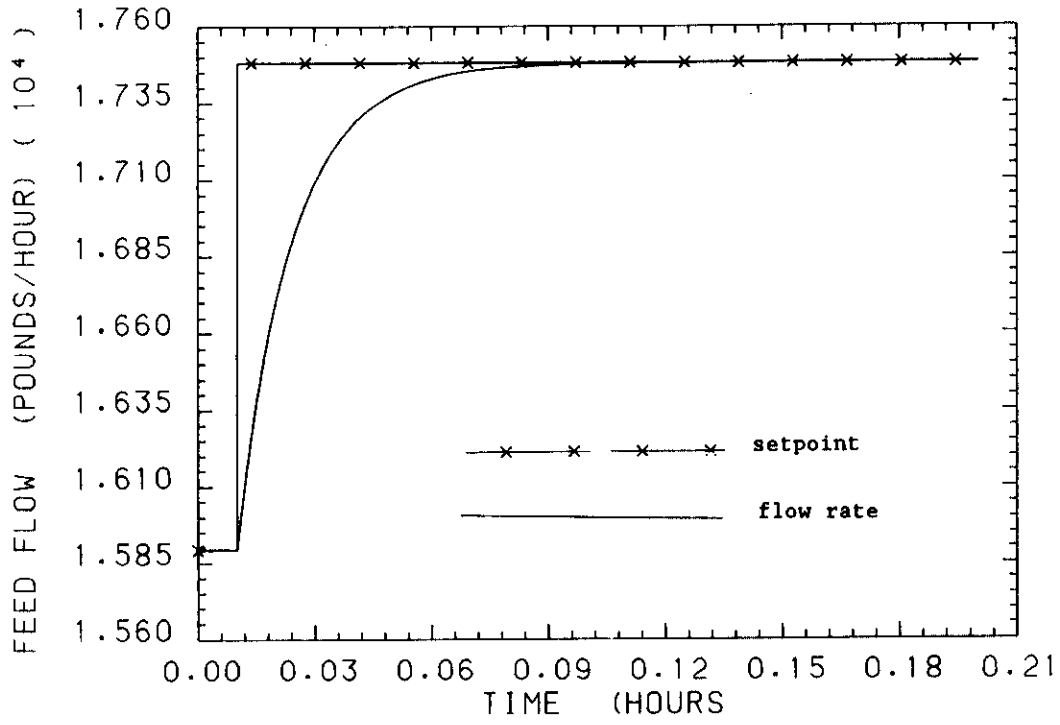

FIGURE 29. Response of Hat to Input Step

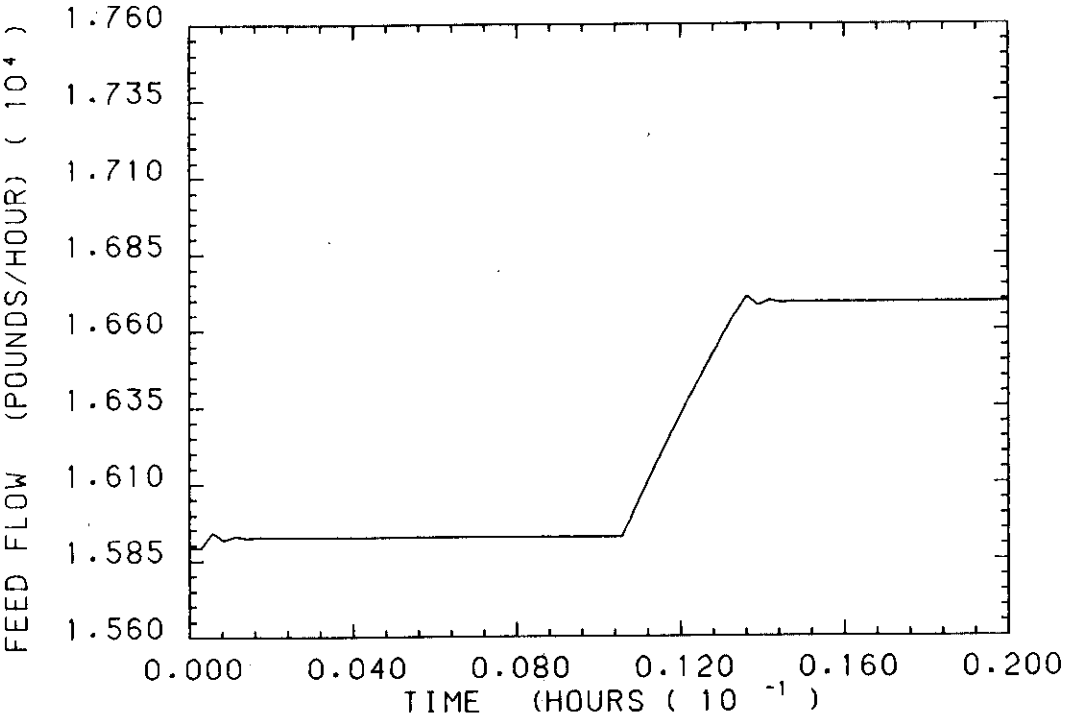

FIGURE 30. Response of Hat to Setpoint Change

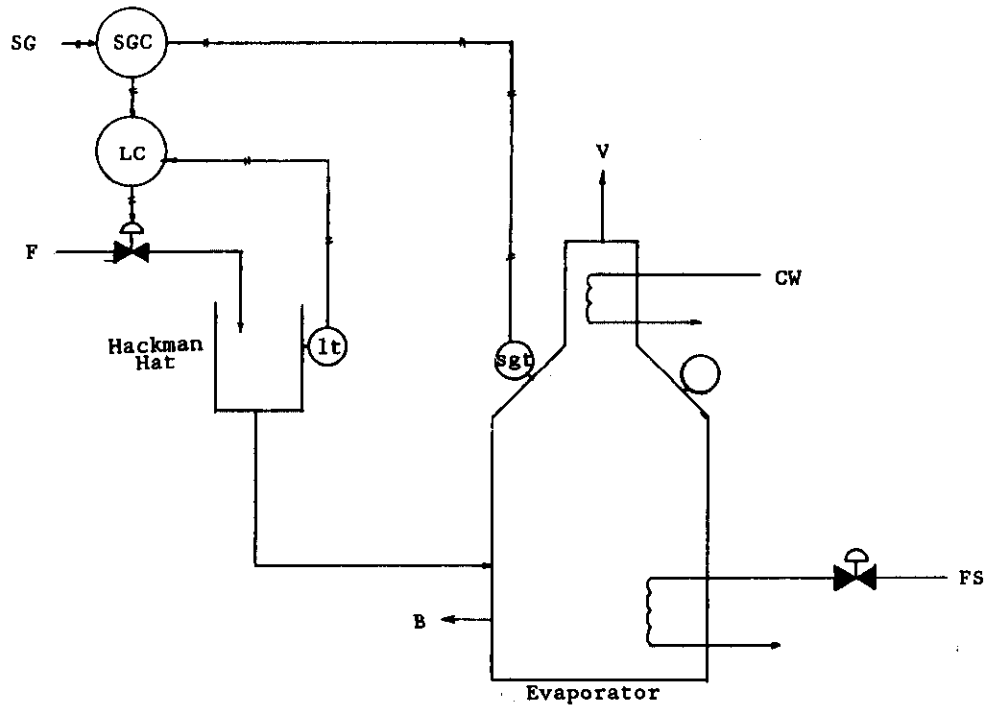

FIGURE 31. Present Control System

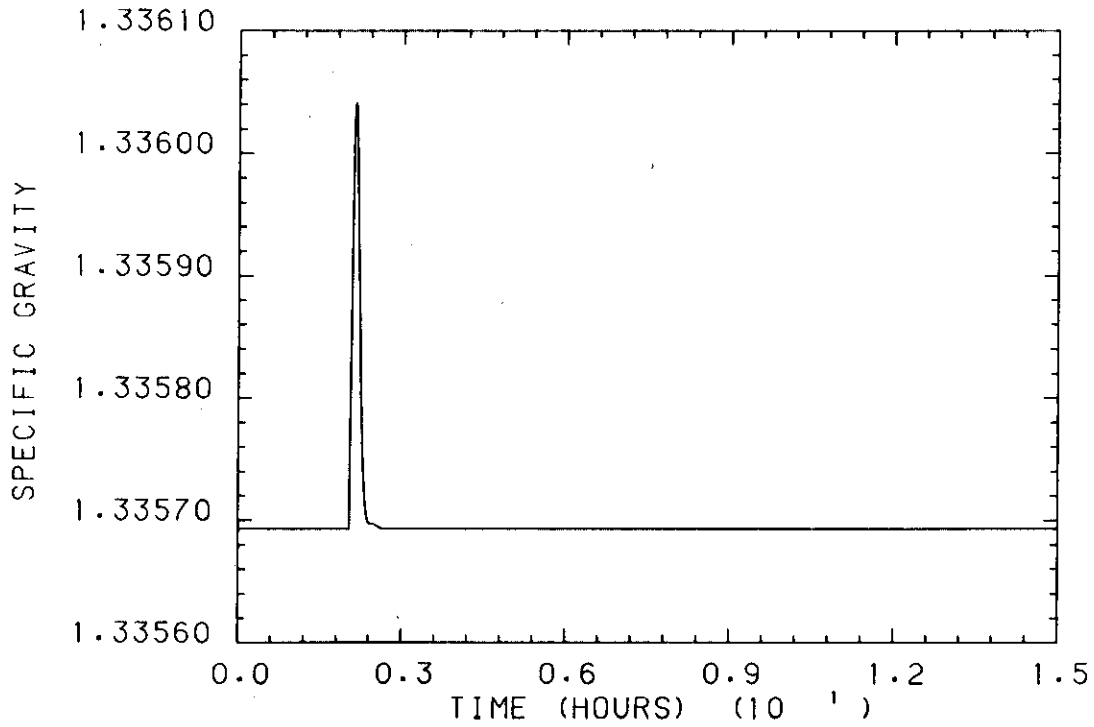

FIGURE 32. Present Controller on Feed Temperature Disturbance

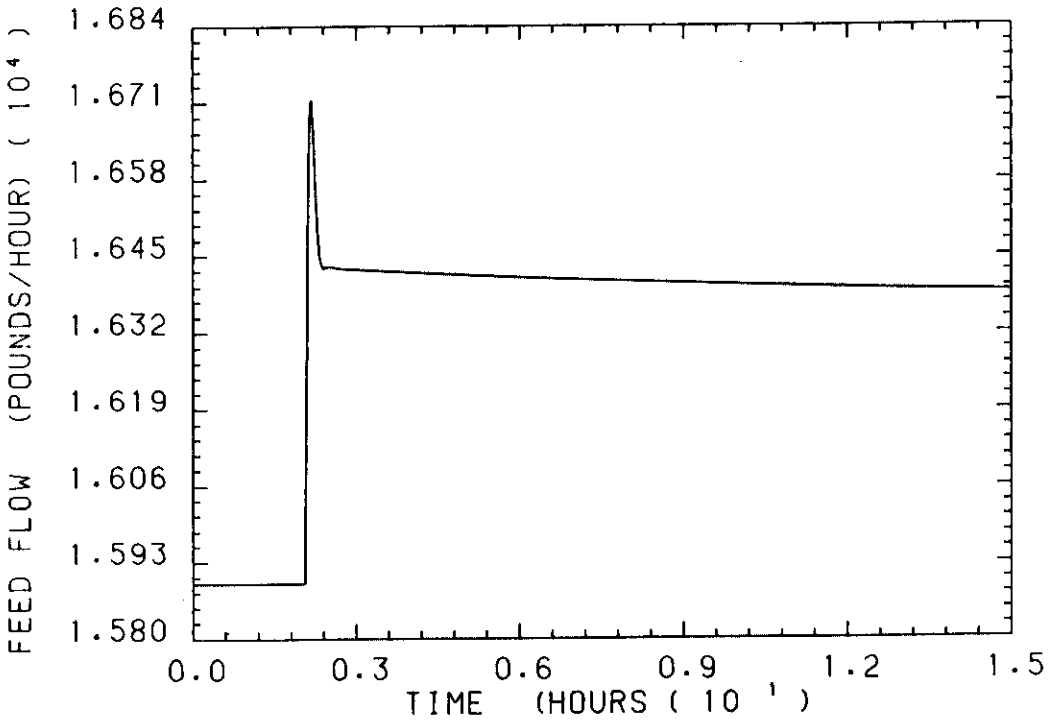

FIGURE 33. Control Action of Present Controller on Feed Temperature Disturbance

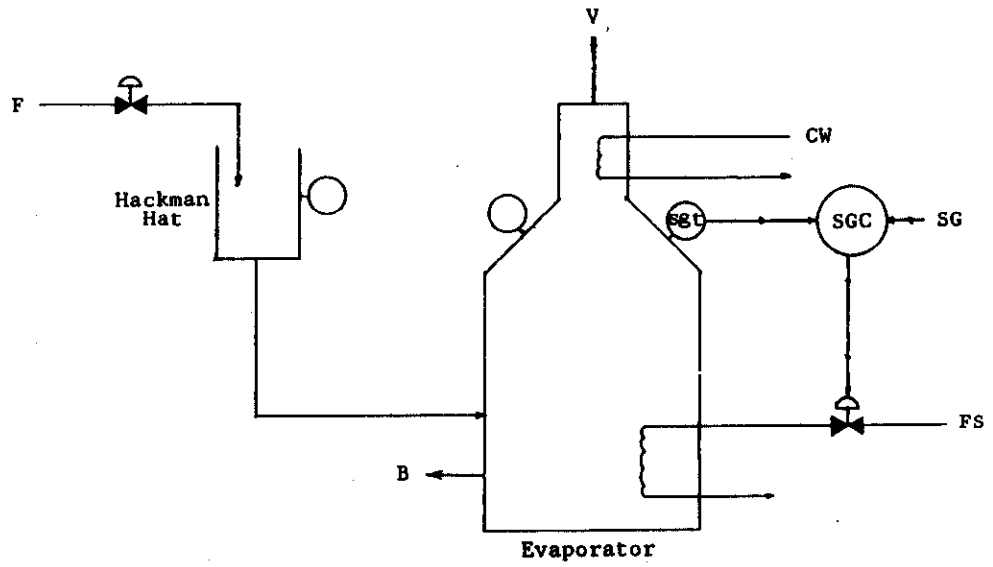

FIGURE 34. Control System Using Steam Flow as the Manipulated Variable

typically operated at or near the maximum steam flow, this system would be very constrained and therefore unusable. If new evaporators are constructed, they should be designed with higher steam flow capabilities. Then the steam controller could be used. This would be a simple way to avoid the complexity added by the Hackman Hat flow controller.

Cascade Controller

The next system to be proposed was a cascade with the evaporator liquid height as the inner, or slave loop controlling the Hackman Hat flow controller, and using a master specific gravity controller. Figure 35 gives a block diagram of this system. This system was more difficult to tune since it had three controllers. The Hackman Hat and evaporator liquid height controllers were proportional-only (P) controllers, as they were inner loops, and a PI controller was used on the outer, specific gravity controller to eliminate steady-state offset.

In order to make the Pattern Search of reasonable size, the inner gains were picked and the Pattern Search was done only on the specific gravity controller. The same tuning parameter as above (ITAE + CONAC) was used for this search. The two inner gains were varied, and the tuning constant, β was chosen for each set of inner gains. The best response was obtained by setting the Hackman Hat flow controller gain to 300 and the height controller gain to 10. The specific gravity controller gain and integral time were chosen as -639.0 and 0.1385 hours, respectively. The response of this system is shown in Figure 36, and the controller actions are shown in Figures 37 and 38, with Figure 37 showing the response of the height controller, and Figure 38 showing the response of the hat controller.

This system can be tuned to perform as well as the original system, but it is very difficult to tune. It does not seem worthwhile to add the greater complexity of the inner loop since there is no gain in performance and tuning is made much more difficult.

Combination Controller

The next attempt was to make the manipulated variable a combination of both steam and feed flows. A block diagram is given in Figure 39. This is done by adding a ratio controller so that the steam flow "tracks" the feed flow, i.e., if the feed flow is increased by 50 lb/hr, the steam flow is increased by a ratio times 50 lb/hr. The ratio was chosen to be -1.035, which is the ratio between the steady-state gains of the effect on the specific gravity of the feed and steam flows. Unfortunately, the addition

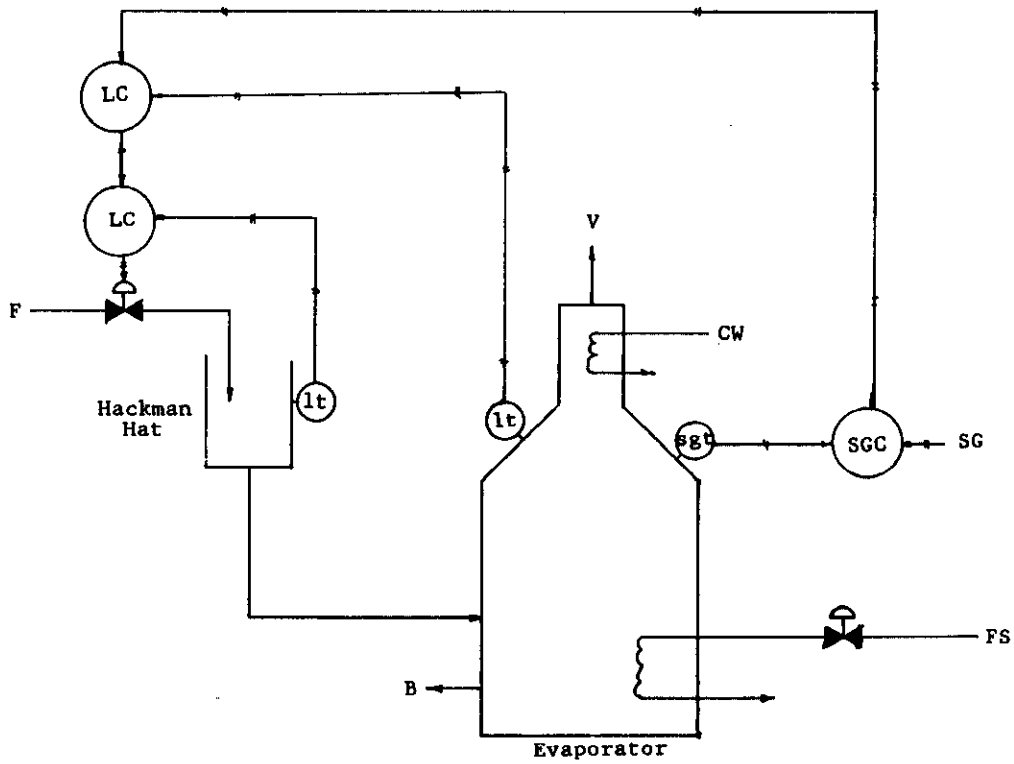

FIGURE 35. Cascade Control System

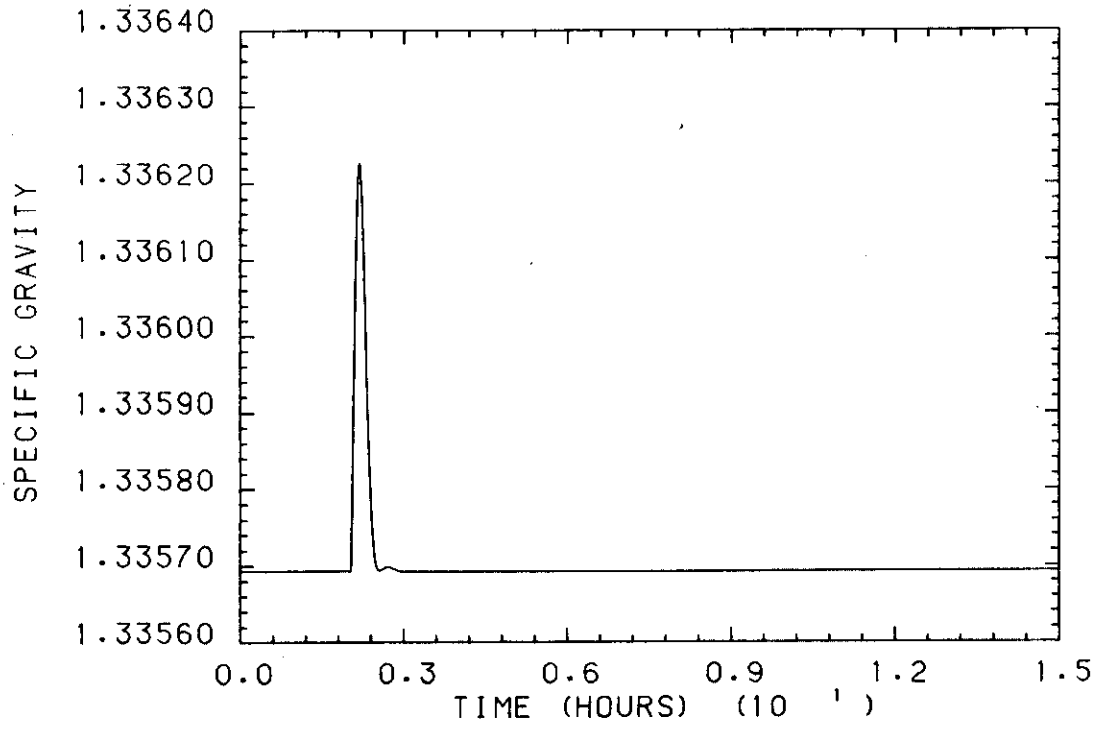

FIGURE 36. Cascade Controller on Feed Temperature Disturbance

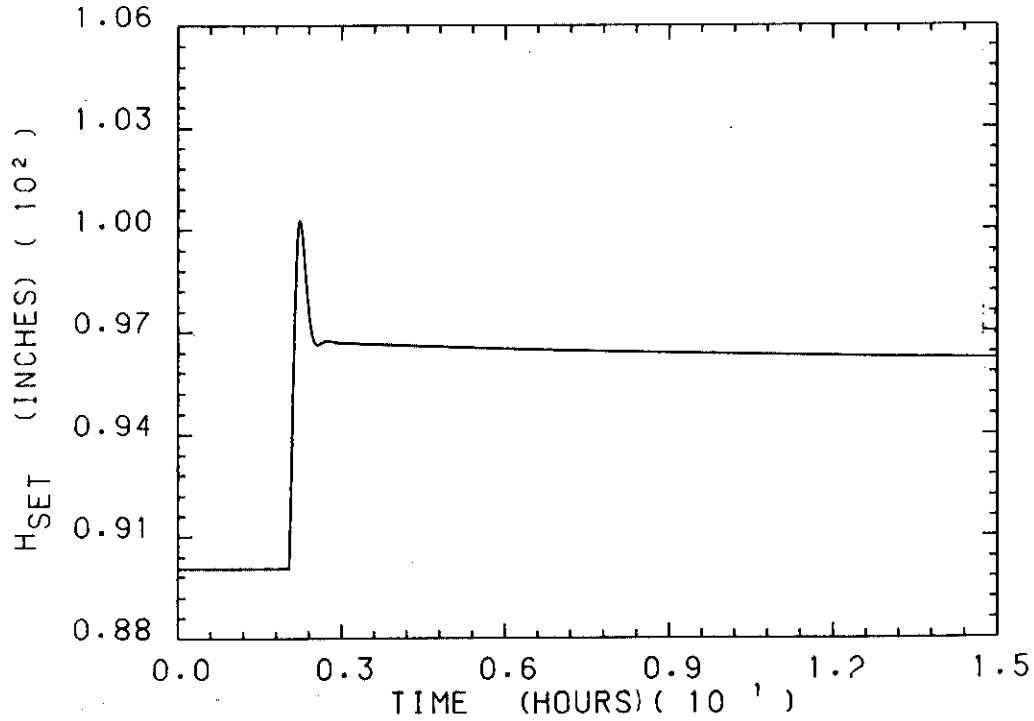

FIGURE 37. Control Action of Cascade Controller on Feed Temperature Disturbance

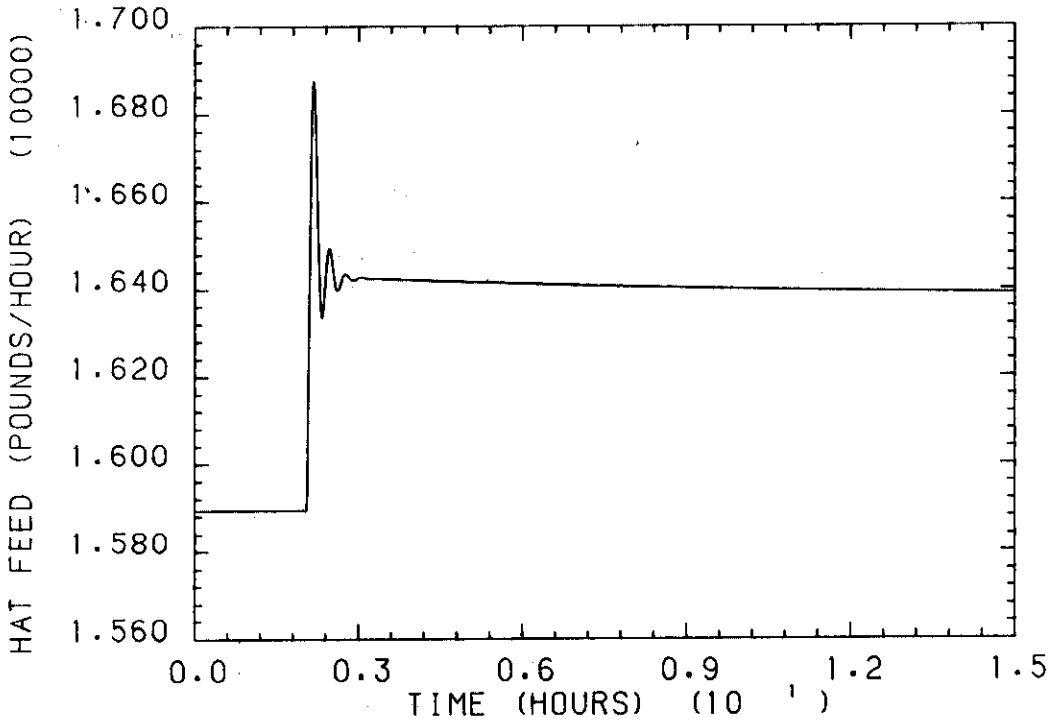

FIGURE 38. Control Action of Cascade Controller on Feed Temperature Disturbance

of the steam flow to the controller slowed the response slightly, which is undesirable. This change also proved to be useless. The response of the system to the new manipulated variable is compared to that of the original system in Figure 40.

Since the evaporator has only one specified variable, that being specific gravity, and the cascade controllers show no benefit over the present single loop control, the preliminary recommendation is to continue with the present control organization.

RELATIVE GAIN ANALYSIS

The primary control variable for the evaporator is specific gravity. However, to help stabilize the system, the possible use of multivariable control of various intermediate variables was considered. Relative gain analysis (RGA) was used to determine possible controller pairings to be used for this purpose. RGA is a method for determining the steady-state interaction between a given pairing of inputs and outputs.[10]

The response of the system to five percent disturbances in steam and feed flows was used to calculate the steady-state gains for use in the RGA calculations. They are given in Table 7. All possible controller pairings were tested using RGA; the relative gain arrays are given in Tables 8 through 22.

Any control variable pairings must necessarily include specific gravity, as it is the primary control variable. Unfortunately, the only variables that do not exhibit significant steady-state interaction with specific gravity are pressure and vapor flow, as shown in Tables 8 and 15.

Since vapor flow is a direct function of pressure, controlling pressure would also control vapor flow. However, controlling the vapor rate would slow the response of the system tremendously, since the evaporator changes the concentration of the liquid by boiling off excess water. Therefore, the use of multivariable control is rejected.

NOISE

As can be seen from the actual process data in Figure 41, there is a considerable amount of noise in the system. From times when the process was under manual control, the noise level in the specific gravity signal was determined to be plus or minus 0.003. Since the characteristic frequencies (if any) could not be determined, a computer-generated random number was used to represent the noise. The simulated noise signal is shown in Figure 42. This is

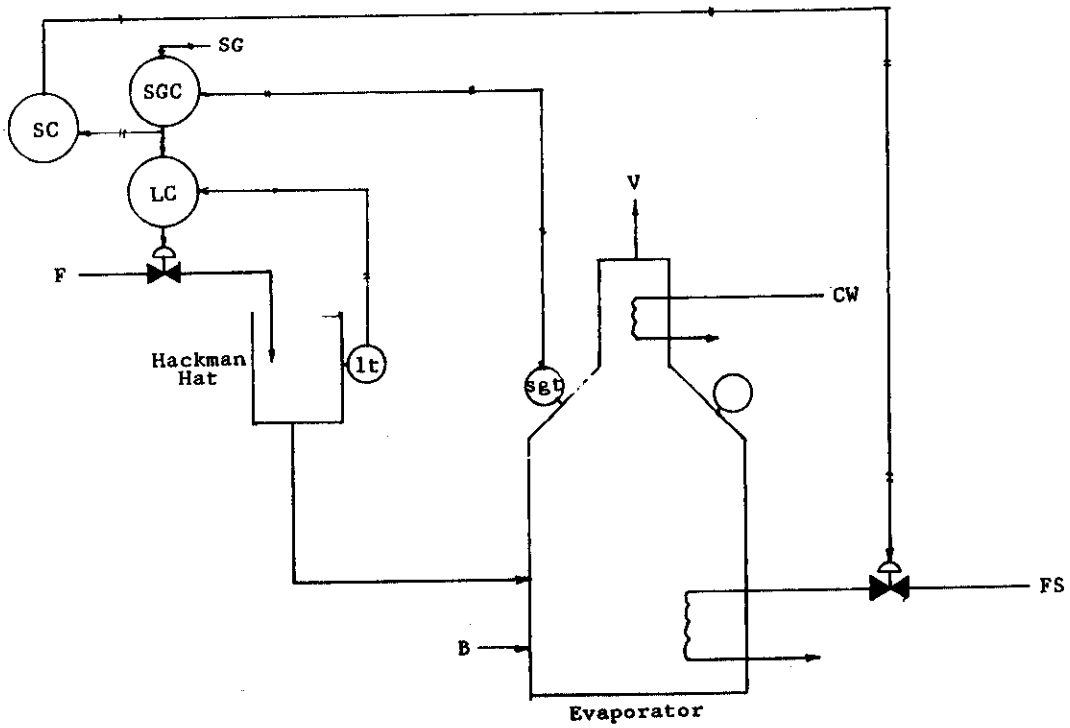

FIGURE 39. Control System Using Feed and Steam Flows as Manipulated Variable

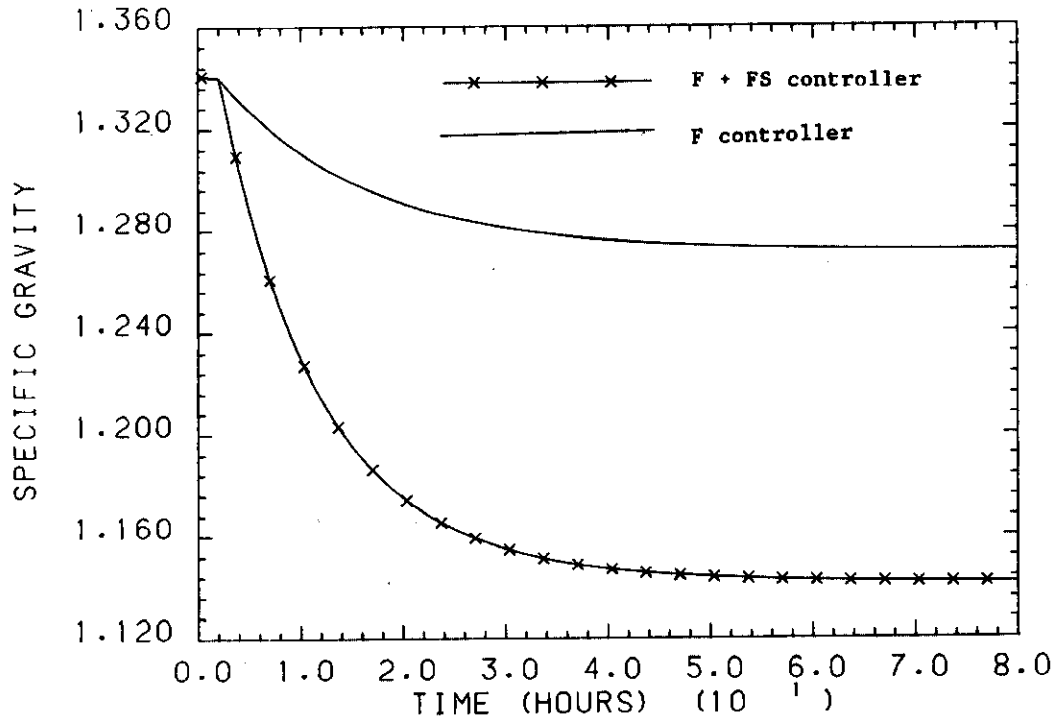

FIGURE 40. Comparison of System Response to Step Input from Original Control System and Dual Flow Controller

TABLE 7

Process Gain Matrix for Evaporator

	Feed Flow	Steam Flow
Pressure	-1.2162×10^{-5}	3.3160×10^{-4}
Temperature	-5.0820×10^{-3}	4.7915×10^{-2}
Specific Gravity	-1.2187×10^{-4}	1.2617×10^{-4}
Liquid Height	1.7213×10^{-4}	-2.7809×10^{-4}
Vapor Flow	-4.4115×10^{-2}	1.2368
Bottoms Flow	1.0476	-1.2376

TABLE 8

Relative Gain Matrix for Pressure and Specific Gravity

	Feed Flow	Steam Flow
Pressure	-0.04	1.04
Specific Gravity	1.04	-0.04

TABLE 9

Relative Gain Matrix for Pressure and Liquid Height

	Feed Flow	Steam Flow
Pressure	0.06	0.94
Liquid Height	0.94	0.06

TABLE 10

Relative Gain Matrix for Pressure and Temperature

	Feed Flow	Steam Flow
Pressure	-0.04	0.96
Temperature	0.96	-0.04

TABLE 11

Relative Gain Matrix for Pressure and Vapor Flow

	Feed Flow	Steam Flow
Pressure	36.4	-35.4
Vapor Flow	-35.4	36.4

TABLE 12

Relative Gain Matrix for Pressure and Bottoms Flow

	Feed Flow	Steam Flow
Pressure	-0.05	1.05
Bottoms Flow	1.05	-0.05

TABLE 13

Relative Gain Matrix for Specific Gravity and Liquid Height

	Feed Flow	Steam Flow
Specific Gravity	2.78	-1.78
Liquid Height	-1.78	2.78

TABLE 14

Relative Gain Matrix for Specific Gravity and Temperature

	Feed Flow	Steam Flow
Specific Gravity	-10.2	11.2
Temperature	11.2	-10.2

TABLE 15

Relative Gain Matrix for Specific Gravity and Vapor Flow

	Feed Flow	Steam Flow
Specific Gravity	1.04	-0.04
Vapor Flow	-0.04	1.04

TABLE 16

Relative Gain Matrix for Specific Gravity and Bottoms Flow

	Feed Flow	Steam Flow
Specific Gravity	8.10	-7.10
Bottoms Flow	-7.10	8.10

TABLE 17

Relative Gain Matrix for Liquid Height and Temperature

	Feed Flow	Steam Flow
Liquid Height	-1.40	2.40
Temperature	2.40	-1.40

TABLE 18

Relative Gain Matrix for Temperature and Vapor Flow

	Feed Flow	Steam Flow
Temperature	1.03	-0.03
Vapor Flow	-0.03	1.03

TABLE 19

Relative Gain Matrix for Temperature and Bottoms Flow

	Feed Flow	Steam Flow
Temperature	4.96	-3.96
Bottoms Flow	-3.96	4.96

TABLE 20

Relative Gain Matrix for Liquid Height and Vapor Flow

	Feed Flow	Steam Flow
Liquid Height	1.06	-0.06
Vapor Flow	-0.06	1.06

TABLE 21

Relative Gain Matrix for Liquid Height and Bottoms Flow

	Feed Flow	Steam Flow
Liquid Height	-2.72	3.72
Bottoms Flow	3.72	-2.72

TABLE 22

Relative Gain Matrix for Vapor Flow and Bottoms Flow

	Feed Flow	Steam Flow
Vapor Flow	-0.04	1.04
Bottoms Flow	1.04	-0.04

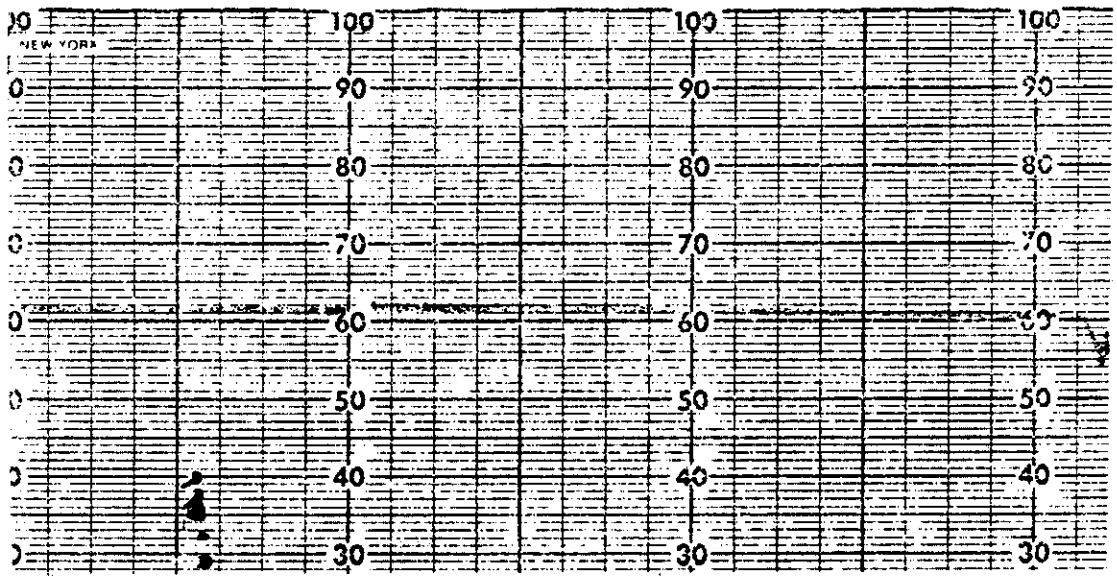

Specific Gravity is Reading Divided by 100 Plus a Constant

FIGURE 41. Actual Process Data Showing Noise Signal

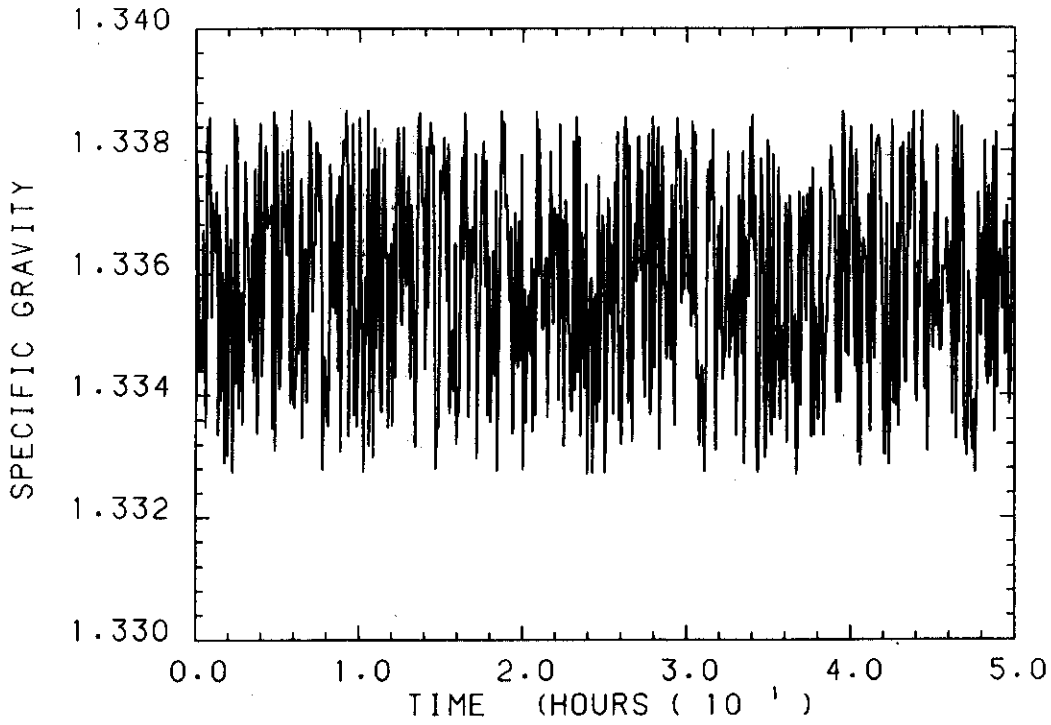

FIGURE 42. Simulated Noise Signal

a worst-case example, as it is much easier to design a filter to reduce a noise signal if its frequency is known. The addition of such a large noise signal makes control of the process very difficult. Only the original control system was used in this phase of the study.

The two most difficult problems that the noise causes are decreased stability and "bang-bang" valve manipulation, where the control valve opens and shuts repeatedly. This is undesirable, both from an operational and from a maintenance point of view. The controllers were tuned by hand, with the hat controller gain set at 660.0 and the specific gravity controller gain and integral time chosen as -620.0 and 0.5 hours. The response is shown in Figure 43. The control action is shown in Figure 44.

An integral-only (I) controller was applied to the system, but the response of the system was too slow. The gain for the controller was chosen as -50.0. The response of this system to a 20 degree increase in feed temperature is given in Figure 45.

Filters

The obvious solution to this problem is the use of a filter to decrease the noise. The drawbacks of a filter are that it increases the order of the system and slows the response, both decreasing stability.

First Order Filter

A first order filter was implemented of the form

$$dX(i) = -a * x(i-1) + b * M(i-1-n)$$

$$X(i) = X_{ss} + \Sigma dX(i)$$

$$n = N/dt$$

$$alpha = \exp(-dt/T)$$

$$a = -alpha$$

$$b = K(1 - alpha)$$

where X(i) is the current value of the output, dX(i) is the effect on the output of the input, X_{ss} is the steady-state value of the output, N is the dead time, expressed in hours, n is the integer dead time, T is the time constant of the particular relation, expressed in hours, and a and b are the difference equation constants.

The filter and the controllers were tuned by hand since the Pattern Search proved to be very noise-sensitive. The oscillation caused by the noise was so high that it masked the deviation of the specific gravity from the setpoint. The response of the system is shown in Figure 46, the readout of the specific gravity instrument is shown in Figure 47, and the controller action is shown in Figure 48.

One problem with a situation such as this, is that it is difficult to say what is the best control. There is a tradeoff between keeping the deviation from setpoint small and reducing the control valve oscillation. An alternate tuning point is given, showing this tradeoff. The gain of the hat controller is identical in both cases, at 660.0. The first uses a filter time constant of 0.1333 hours and a master controller gain and integral time of -3000.0 and 0.7 hours. The alternative tuning uses a filter time constant of 0.3333 hours, and a master controller gain and integral time of -500.0 and 1.5 hours. The response of the alternately tuned system to the feed temperature increase is shown in Figure 49 and the controller action appears in Figure 50.

Notice that the higher filter time constant decreases the noise, but delays the response of the system, necessitating a greater integral time and smaller gain in the controller, which slows its response. The actual tuning choice will depend on the amount of control valve oscillation and deviation from setpoint that can be tolerated. The gain of the controller can be increased, which will lessen the initial overshoot due to the disturbance but increase the "steady-state" oscillation due to noise.

Second Order Filter

Next, a second order filter was tried, using two identical time constants. This filter should show greater noise attenuation, but unfortunately it also delays the system response greatly. The second order filter was implemented in difference equation form. The equation is

$$X(i) = -a_1 * X(i-1) - a_2 * X(i-2) + b_1 * M(i-1-n) + b_2 * M(i-2-n)$$

$$a_1 = -2 * \text{alpha}$$

$$a_2 = \text{alpha}^2$$

$$b_1 = K\left[1 - \text{alpha}\ (1 + T/\tau)\right]$$

$$b_2 = K\left[\text{alpha}\ (\text{alpha} - 1 - T/\tau)\right]$$

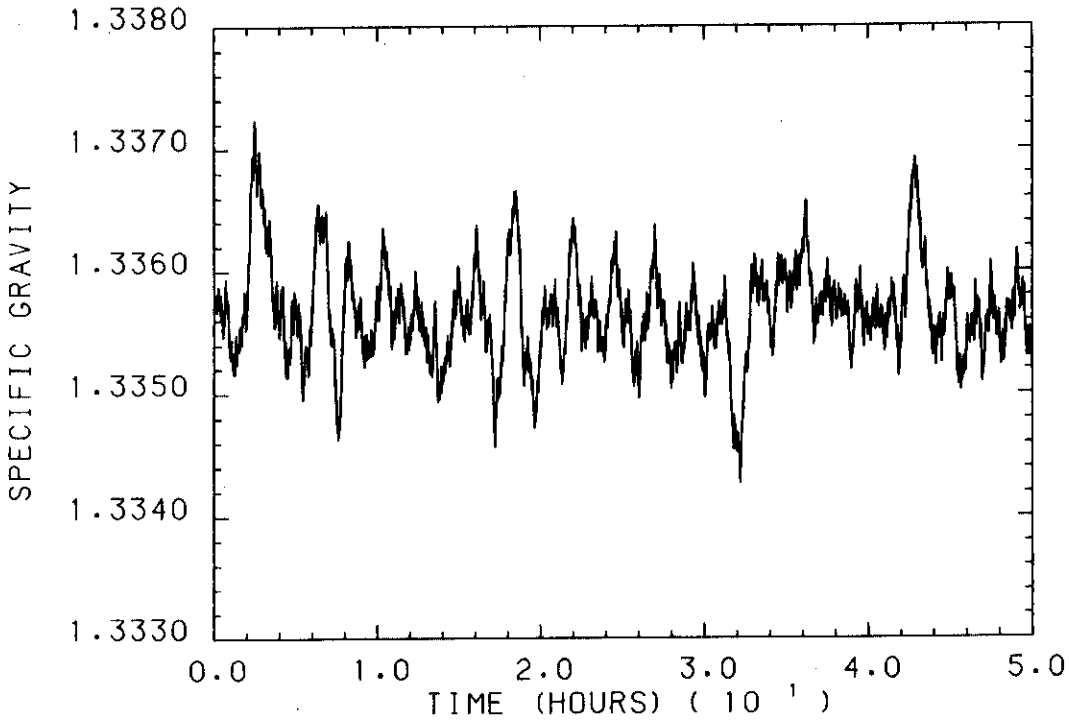

FIGURE 43. Original Controller on Feed Temperature Disturbance with Noise

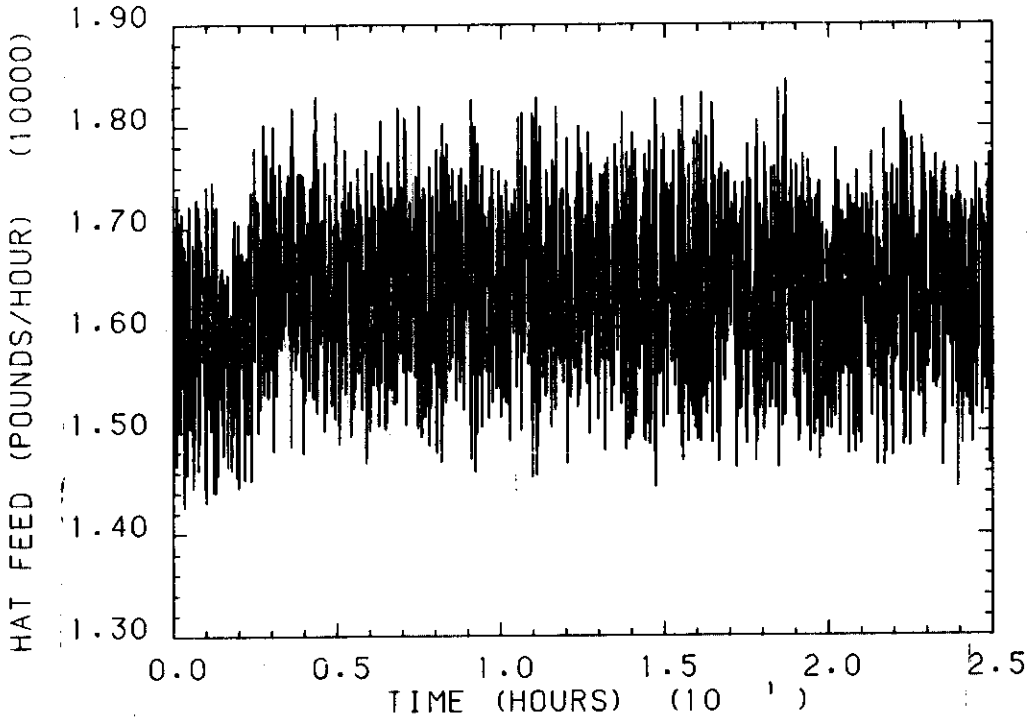

FIGURE 44. Control Action of Original Controller on Feed Temperature Disturbance with Noise

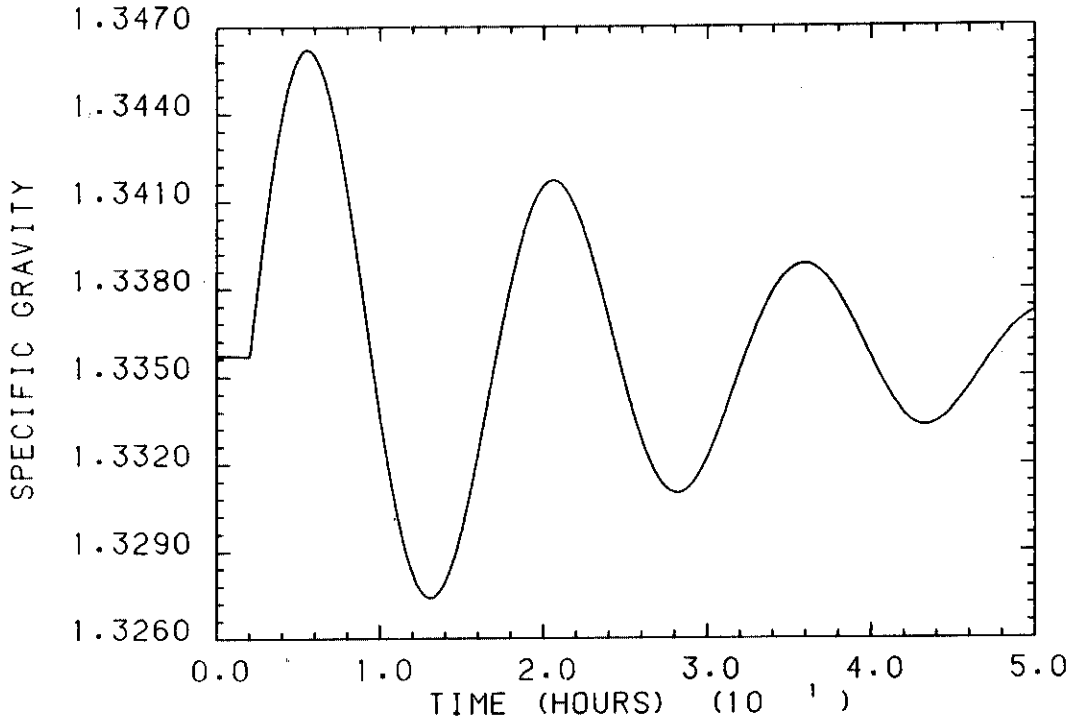

FIGURE 45. I Controller on Feed Temperature Disturbance with Noise

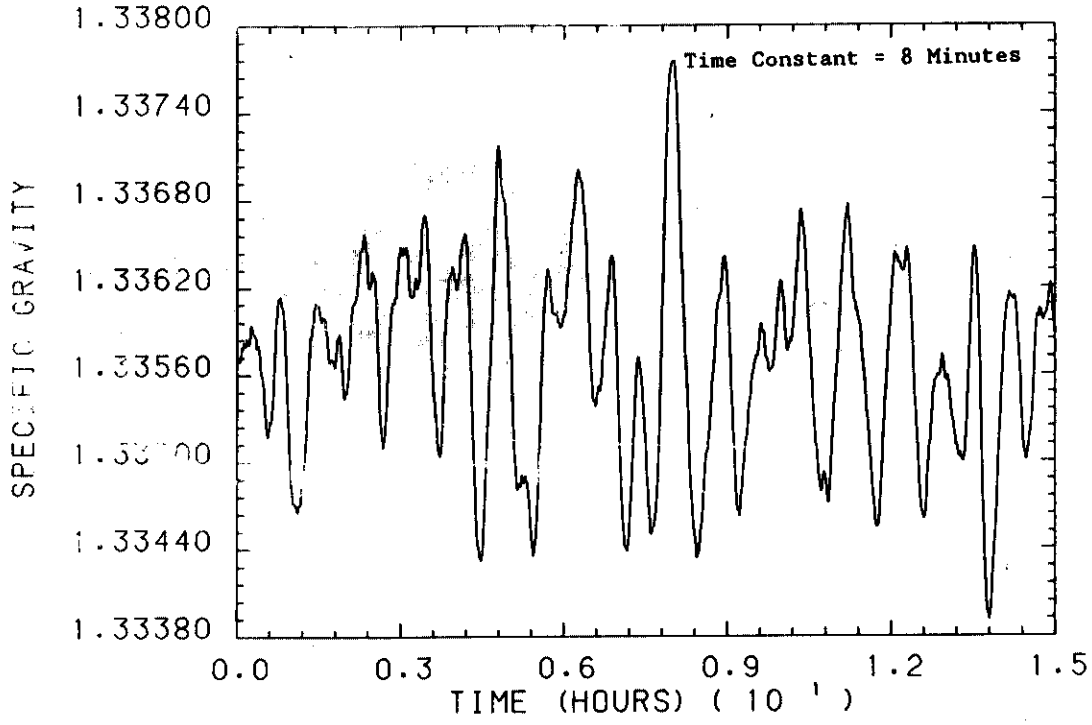

FIGURE 46. Response Using First Order Filter

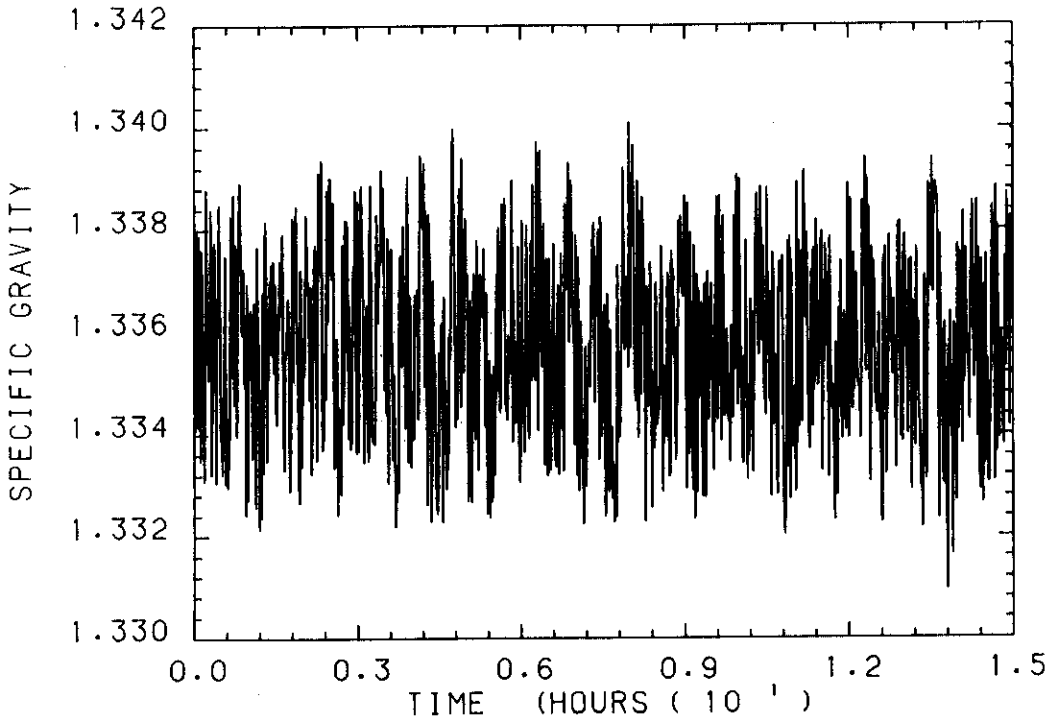

FIGURE 47. Signal from Specific Gravity Instrument

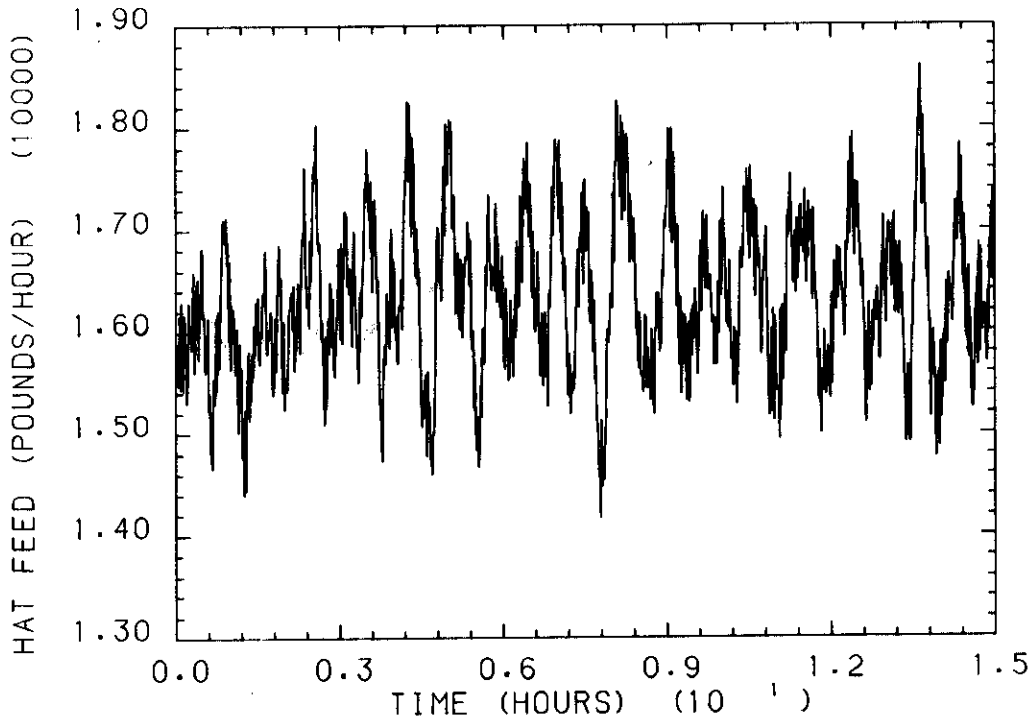

FIGURE 48. Control Action Using First Order Filter

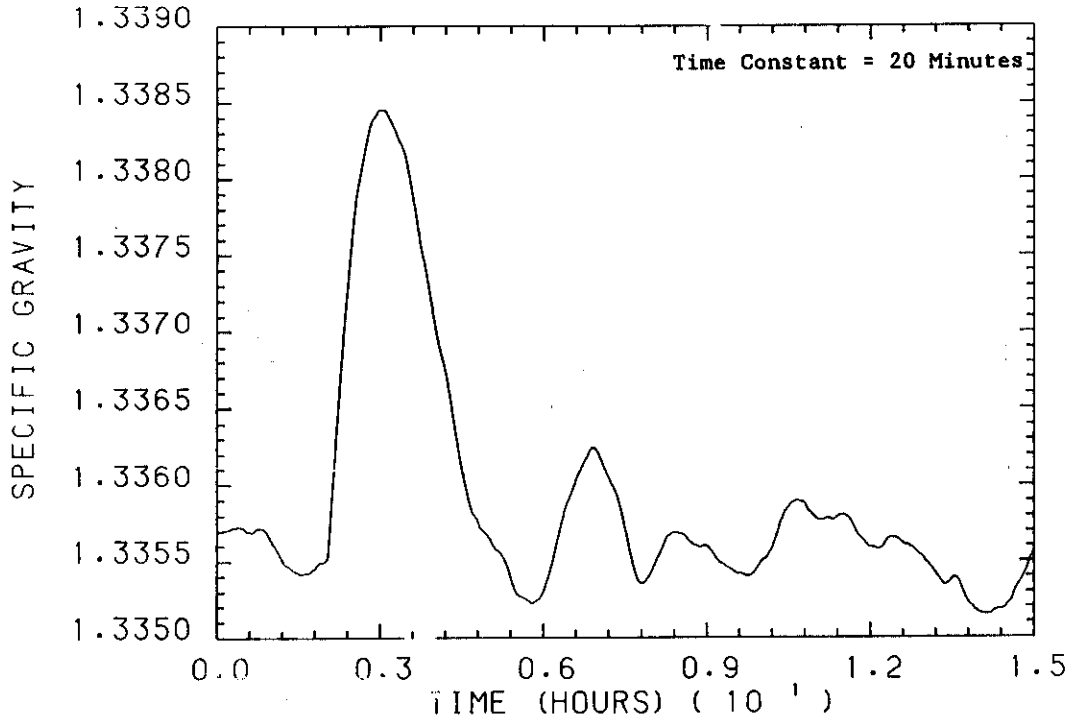

FIGURE 49. Alternate Response Using First Order Filter

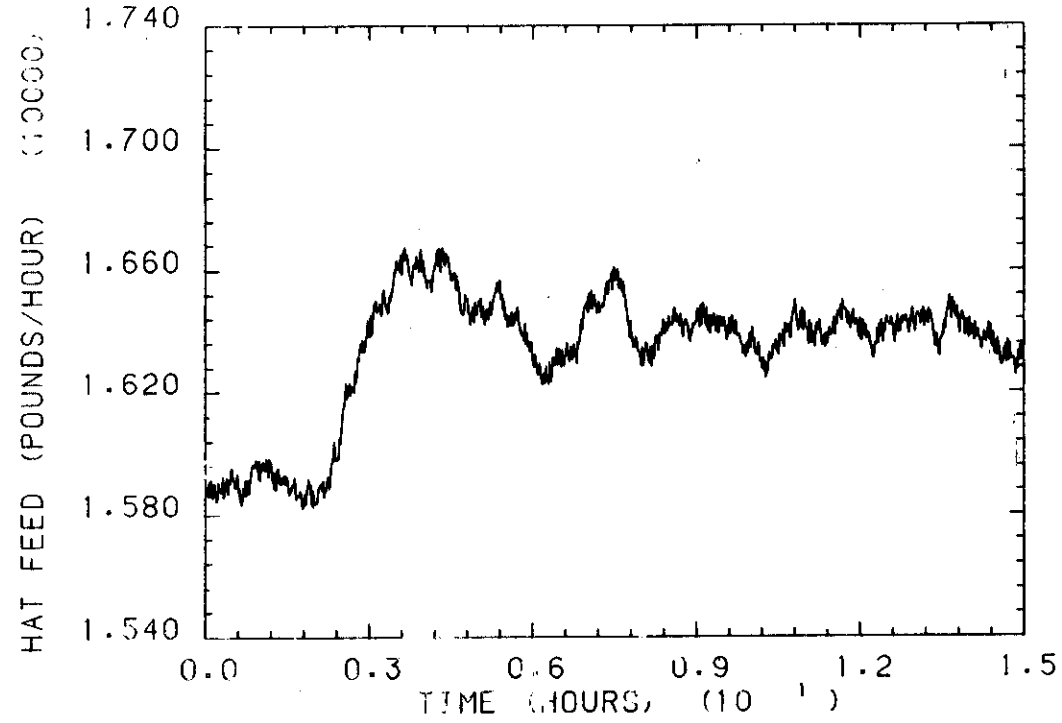

FIGURE 50. Alternate Control Action Using First Order Filter

where X is the output, M is the input, and n is the integer dead time.

The filter time constant was chosen as 0.3333 hours and the system was tuned by hand, as was the first order filter. The hat controller gain was chosen as 660.0, and the master controller gain and integral times were -500.0 and 5.0 hours. The response of the system using the second order filter with the above tuning is given in Figure 51.

Split Filtering

A small improvement to the control system was made by filtering only the signal to the proportional part of the controller as shown in Figure 52. The responses of the system with complete filtering and with partial filtering are compared in Figure 53. The line with the x's is the split controller. Note that the initial overshoot is slightly less for the split controller, but the difference quickly becomes negligible.

CONCLUSIONS AND RECOMMENDATIONS

The control studies showed that the control algorithm now in use at SRP is the best and simplest available. In this algorithm, the feed flow is used to control the specific gravity of the liquid in the evaporator. The use of a first order filter on the specific gravity transducer signal was found to greatly reduce control valve oscillation caused by noise. There was a small benefit from filtering only the signal to the proportional mode of the controller.

The time constant of the filter should be selected after deciding on the tradeoff between the relative amounts of overshoot and control valve oscillation that can be accepted. Tuning the specific gravity controller should be done using the ITAE + CONAC parameter used in this study. The tuning constant, β, should be selected to give the best possible response.

If it is desired to use the model for control studies for other evaporators, experiments should be undertaken to determine whether the constants in the dissociation equations fit the uranium salt solutions as well as the magnesium salt solutions that they were developed for. If a flowmeter can be found that meets reliability requirements, the Hackman Hat flow control should be replaced. It introduces a first order lag into the system and adds to the difficulty in tuning the system since it has a level controller.

If new evaporators are to be constructed, they should have provision for a much higher steam flow rate, as the evaporators presently run at or near the maximum steam flow rate. This would make it possible to use the steam flow, rather than the feed flow, as the manipulated variable. This would be a good alternative to the system presently used.

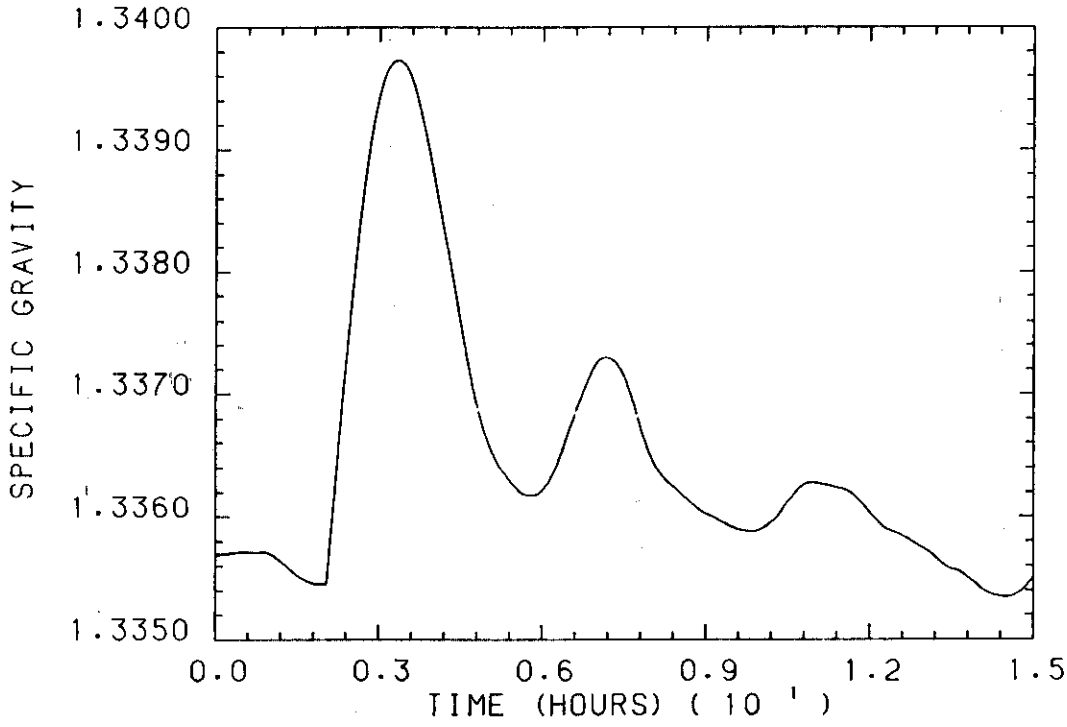

FIGURE 51. Response Using Second Order Filter

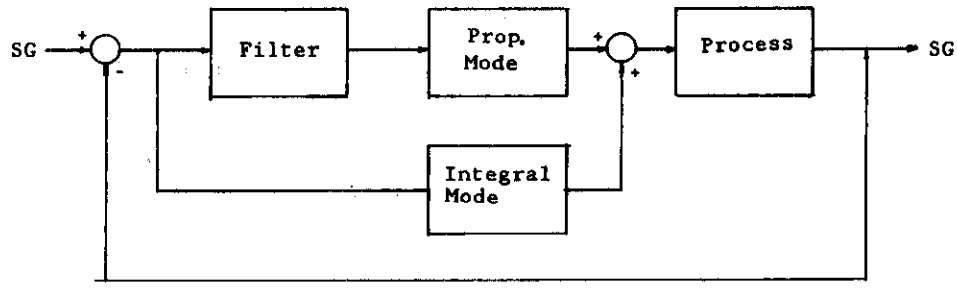

FIGURE 52. Flowchart of Split Filter Control System

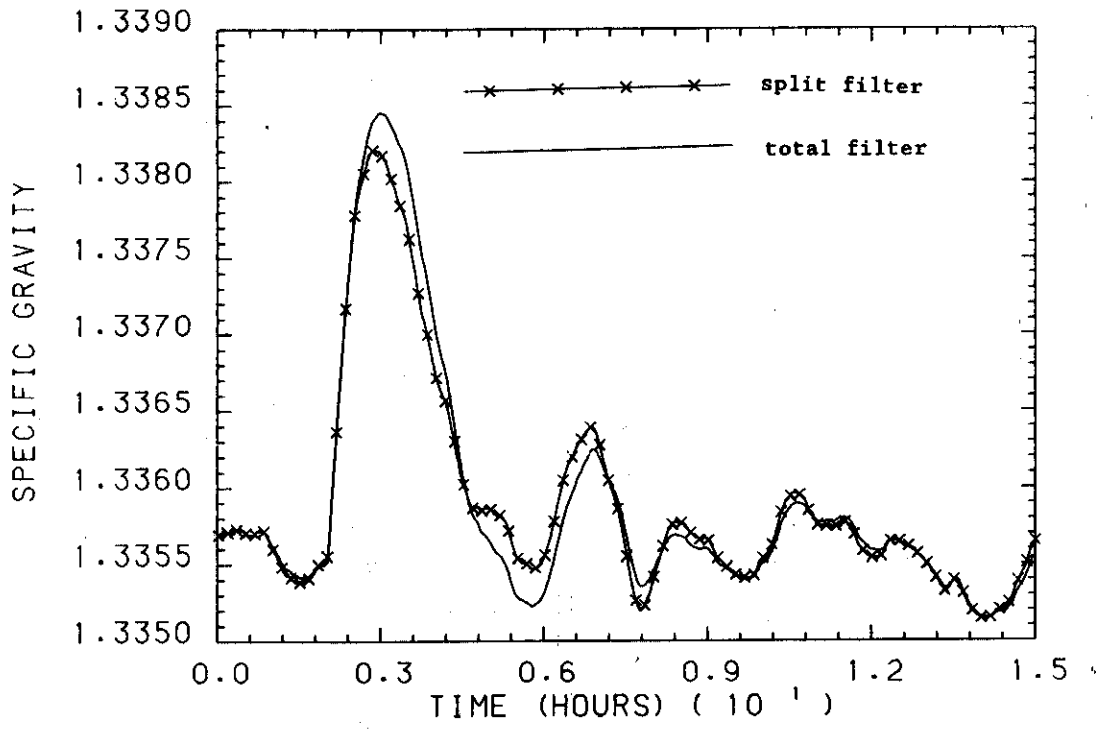

FIGURE 53. Effect of Filtering Only Signal to Proportional Mode

BIBLIOGRAPHY

1. Bacon, D. W. and G. L. Howe. "Statistical Evaluation and Design of an Evaporator Control System." The Canadian Journal of Chemical Engineering, 50, pp. 119-127, February 1972.

2. Harvey, D. J. and J. R. Fowler. "Dynamic Process Modeling of a Quadruple Effect Evaporator System." Chemical Engineering Progress, April 1976.

3. Chen, C. S., R. D. Carter, W. M. Miller, and J. A. Wheaton. "Computer Control for Evaporators." Food Engineering, pp. 82-83, February 1981.

4. Kleinpeter, J. A. and R. E. C. Weaver. "Multivariate Control of a Phase Separator Process." AIChE Journal, 17: 3, pp. 513-519, March 1971.

5. Rich, S. E., V. J. Laio, and R. E. C. Weaver. "Simulation Model Characteristics and the Performance of Multivariate Control Schemes."

6. Newell, R. B. and D. G. Fisher. "Model Development, Reduction, and Experimental Evaluation for an Evaporator." Industrial Engineering Chemical Process Design and Development, 11: 2, pp. 213-221 (1972).

7. Newell, R. B., D. G. Fisher, and D. E. Seborg. "Computer Control Using Optimal Multivariate Feedforward — Feedback Algorithms." AIChE Journal, 18: 5, pp. 976-984, September 1972.

8. Fisher, D. G. and D. E. Seborg. "Advanced Computer Control Improves Process Performance." Instrumentation Technology, pp. 71-77, September 1973.

9. Thompson, B. E., J. J. Derby, E. H. Stalzer, R. M. Counce, R. T. Jubin, and R. E. Barker. "Vapor-Liquid Equilibrium of the $Mg(NO_3)_2$ - HNO_3 - H_2O System." ORNL/MIT-360 (1983).

10. Deshpande, P. D. and R. H. Ash. "Elements of Computer Process Control with Advanced Control Applications." Instrument Society of America, pp. 293-302 (1981).

11. PATERN, IBM Share Program Library, LSU-PATE, SDA3552 (1965).

LIST OF SYMBOLS

B	-	Bottoms flow rate, lb/hr
C	-	Uranium concentration, g/L
C(t)	-	Manipulated variable
Cp	-	Heat capacity, BTU/lb/°F
Cp_f	-	Heat capacity of feed, BTU/lb/°F
F	-	Feed flow rate, lb/hr
F_s	-	Steam flow rate, lb/hr
H	-	Height of liquid in evaporator, inches
HO	-	Height of weir above bottom in evaporator, inches
Ka	-	Equilibrium constant
K_h	-	Valve constant for bottoms flow, lb/hr in.
K_{hat}	-	Valve constant for Hackman Hat flow, lb/hr in.
M	-	Mass of liquid in evaporator, lb
N	-	Dead time, hr
Na	-	Normality of acid in evaporator
P_a	-	Equilibrium vapor pressure of acid, inches water
P_c	-	Pressure in condenser, inches water
P_e	-	Pressure at liquid surface in evaporator, inches water
P_w	-	Equilibrium vapor pressure of water, inches water
R	-	Gas constant
T	-	Temperature of liquid in evaporator, °F
T_f	-	Temperature of feed, °F
V	-	Vapor flow rate, lb/hr
X	-	Output of difference equation
X_{ss}	-	Value of X at steady state
a	-	Difference equation constant
b	-	Difference equation constant
dH	-	Heat of reaction
h	-	Height of liquid in Hackman Hat, inches
n	-	Integer dead time
t	-	Time, hr
x_a	-	Analytical mole fraction of acid
x_s	-	Analytical mole fraction of salt

LIST OF SYMBOLS, Contd

x_w - Analytical mole fraction of water

x'_a - Mole fraction of undissociated acid

x'_{a+} - Mole fraction of hydrogen ion

x'_w - Mole fraction of undissociated water

x'_- - Mole fraction of nitrate ion

α - Extent of dissociation

β - Tuning constant

γ'_a - Activity coefficient of undissociated acid

γ'_w - Activity coefficient of undissociated water

Θ - Dead time, hr

λ_s - Heat of vaporization of steam, BTU/lb

λ_v - Heat of vaporization of vapor, BTU/lb

ρ - Specific gravity of liquid in evaporator

τ - Time constant, hr

DOE Form RA-426
(10/80)

U.S. DEPARTMENT OF ENERGY

OMB NO. 038-R0190

DOE AND MAJOR CONTRACTOR RECOMMENDATIONS FOR ANNOUNCEMENT AND DISTRIBUTION OF DOCUMENTS

See Instructions on Reverse Side

1. DOE Report No.	2. Contract No.	3. Subject Category No.
DP-1690	DE-AC09-76SR00001	

4. Title
PROCESS CONTROL FOR A CONTINUOUS URANYL NITRATE EVAPORATOR

5. Type of Document ("x" one)
- ☒ a. Scientific and technical report
- ☐ b. Conference paper: Title of conference _____
  Date of conference _____
  Exact location of conference _____ Sponsoring organization _____
- ☐ c. Other (specify planning, educational, impact, market, social, economic, thesis, translations, journal article manuscript, etc.)

6. Copies Transmitted ("x" one or more)
- ☒ a. Copies being transmitted for standard distribution by DOE–TIC.
- ☐ b. Copies being transmitted for special distribution per attached complete address list.
- ☐ c. Two completely legible, reproducible copies being transmitted to DOE–TIC. (Classified documents, see instructions)
- ☐ d. Twenty-seven copies being transmitted to DOE–TIC for TIC processing and NTIS sales.

7. Recommended Distribution ("x" one)
- ☒ a. Normal handling (after patent clearance): no restraints on distribution except as may be required by the security classification.

Make available only ☐ b. To U.S. Government agencies and their contractors. ☐ c. within DOE and to DOE contractors. ☐ d. within DOE. ☐ e. to those listed in item 13 below.

- ☐ f. Other (Specify)

8. Recommended Announcement ("x" one)
- ☒ a. Normal procedure may be followed. ☐ b. Recommend the following announcement limitations:

9. Reason for Restrictions Recommended in 7 or 8 above.
- ☐ a. Preliminary information. ☐ b. Prepared primarily for internal use. ☐ c. Other (Explain)

10. Patent, Copyright and Proprietary Information

Does this information product disclose any new equipment, process or material? ☒ No ☐ Yes If so, identify page nos. _____

Has an invention disclosure been submitted to DOE covering any aspect of this information product? ☒ No ☐ Yes

If so, identify the DOE (or other) disclosure number and to whom the disclosure was submitted.

Are there any patent-related objections to the release of this information product? ☒ No ☐ Yes If so, state these objections.

Does this information product contain copyrighted material? ☒ No ☐ Yes

If so, identify the page number _____ and attach the license or other authority for the government to reproduce.

Does this information product contain proprietary information? ☒ No ☐ Yes If so, identify the page numbers _____.

("x" one ☒ a. DOE patent clearance has been granted by responsible DOE patent group.
☐ b. Document has been sent to responsible DOE patent group for clearance.

11. National Security Information (For classified document only; "x" one)

Document ☐ a. does ☐ b. does not contain national security information

12. Copy Reproduction and Distribution

Total number of copies reproduced 159 Number of copies distributed outside originating organization 127

13. Additional Information or Remarks (Continue on separate sheet, if necessary)

14. Submitted by (Name and Position) (Please print or type)
D. Chavis, Senior Supervisor

Organization
Information & Publication Services, SRP, Aiken, SC

Signature Dana Chavis Date 8/30/84

EXTERNAL RELEASE OF TECHNICAL INFORMATION

Description of Material No. DP-1690 Date June 22, 1984

Title: PROCESS CONTROL FOR A CONTINUOUS URANYL NITRATE EVAPORATOR

Author(s) S. F. Peterson and L. P. MacIntyre

Date of Material

( ) Classified DP Report	( ) Classified Paper
(XXX) Unclassified DP Report	( ) Unclassified Paper
( ) Classified Letter	( ) Classified Abstract or Summary
( ) Unclassified Letter	( ) Unclassified Abstract or Summary

Technical Content

Approved by C E Coffey (C. E. Coffey) Date 6/22/84

Classification

Approved by C E Coffey (C. E. Coffey) Date 6/22/84

Approved by C J Banick (AED Classification Officer) Date 6/22/84

Authority

CG-UF-3, Topic 4.3.1

Category if DP Report

Approved by N/A (Supervisor, I&PS) Date

Released by:

A. F. Westerdahl 6/29/84

E. L. Bowser 7/16/84 By phone 7/13 Inf. Ed.

OSR 25-5
(REV 3-83)

E. I. DU PONT DE NEMOURS & COMPANY
INCORPORATED
ATOMIC ENERGY DIVISION
SAVANNAH RIVER PLANT
AIKEN, SOUTH CAROLINA 29808-0001
(TWX: 810-771-2670, TEL: 803-725-6211, WU AUGUSTA, GA.)

CC: J. M. Stogner

June 22, 1984

Mr. A. F. Westerdahl, Chief
Patent Branch
U. S. Department of Energy
Aiken, South Carolina 29808

Dear Mr. Westerdahl:

REQUEST FOR PATENT REVIEW

Please review for patent matter:

DP-1690, "PROCESS CONTROL FOR A CONTINUOUS URANYL NITRATE EVAPORATOR", by S. F. Peterson and L. P. MacIntyre.

If any technical clarification is needed please call C. J. Banick whose Document Review is attached.

Please telephone your comments to the Records Management Office (Ext. 2606) and notify me by signing and returning to C. J. Banick the original of this letter. A copy is provided for your file.

If you decide to pursue a patent on any development covered, I shall be happy to supply additional information required such as appropriate references and the names of persons responsible for the development.

Very truly yours,

J. M. Stogner, Chief Supervisor
Records Management

The above item is approved
for release.

By: C J Banick

A. F. Westerdahl 6/29/84
Date
Chief Patent Branch
DOE-SR

TO: Senior Information Specialist, I&PS, SRL, 773-A DATE: 7-16-84

DOCUMENT NO.: DP-1690 "PROCESS CONTROL FOR A CONTINUOUS URANYL NITRATE EVAPORATOR"

RECEIVED ~~OEA~~ P&ME/SR ON: 6 / 28 / 84

The above referenced document has been reviewed by SR staff and is:

/ XX / Approved for release as written.

/ ___ / Approved for release subject to the following changes:

/ ___ / Not Approved for release.

ADDITIONAL COMMENTS: Needs Distribution page, UC Category Code - Approved by Info put on.

E. J. Bowser

E. L. Bowser, Technical Information Officer, DOE-SR

~~Office of External Affairs~~

Attachment

OSR 25-5
(REV 3-83)

E. I. DU PONT DE NEMOURS & COMPANY
INCORPORATED
ATOMIC ENERGY DIVISION
SAVANNAH RIVER PLANT
AIKEN, SOUTH CAROLINA 29808-0001
(TWX: 810-771-2670, TEL: 803-725-6211, WU AUGUSTA, GA.)

CC: A. F. Westerdahl, DOE-SR
J. M. Stogner

June 22, 1984

TO: J. M. STOGNER

FROM: C. J. BANICK CJB

DOCUMENT REVIEW

Document: DP-1690

Title: PROCESS CONTROL FOR A CONTINUOUS URANYL NITRATE

Author(s): S. F. Peterson and L. P. MacIntyre

Contractual Origin: DE-AC09-76SR00001

Present Classification: Unclassified DP-Report

References:

No items were noted that, in my opinion, should be called to the attention of the DOE for patent consideration.

INTERNAL DISTRIBUTION

Copy No.

1-3. E. L. Bowser, DOE-SR - Dist 2/1/94

4. A. A. Kishbaugh, Wilm
5. A. S. Barab
6. P. E. Dillon
7. F. W. Pardee, Engg Dept

8. J. A. Kelley, SRP
9. W. R. Jacobsen
10. J. W. Joseph
11. L. M. Papouchado
12. J. F. Ortaldo
13. J. T. Buckner, Jr.
14. C. W. Jenkins
15. J. B. Starks
16. D. Malizia
17. J. G. McKibbin
18 C. E. Pickett

19. J. T. Lowe, SRL
20. J. A. Porter
21. C. E. Coffey
22. D. U. Gwost
23-24. S. F. Peterson
25. H. D. Harmon
26. J. R. Wiley
27. R. M. Mobley
28. R. L. Folger
29. R. F. Bradley
30. W. E. Stewart
31. K. A. Saturday
32. W. A. Spencer
33. A. L. Blancett
34. D. A. Boyce
35. **SRL Record Copy**
36-50. SRL File Copies

SPECIAL DISTRIBUTION (Off-Site)

51. Dr. C. E. Moore
Department of Chemical Engineering
University of Tennessee
Knoxville, TN 37996-2200

52. L. P. MacIntyre
Martin Marietta Energy Systems
P. O. Box P, Building K-1200, MS 253
Oak Ridge, TN 37831

DISTRIBUTION

Copy No.

1-3. E. L. Bowser, DOE-SR

4-30. SRL Record Files

31. C. E. Moore, University of Tennessee

32. L. P. MacIntyre, Martin Marietta Energy Systems

33-159. Technical Information Center (for distribution under TID-4500 Category UC-70)